Zinc isotope composition as a tool for tracing sources and fate of metal contaminants in rivers

Anne-Marie Desaulty, Emmanuelle Petelet-Giraud

Zinc isotope composition as a tool for tracing sources and fate of metal contaminants in rivers

A review

DESAULTY Anne-Marie*, PETELET-GIRAUD Emmanuelle

BRGM, F-45060, Orléans, France

* Corresponding author, e-mail address: am.desaulty@brgm.fr

Abstract

Zinc is a ubiquitous metal, acting both as an essential and a toxic element to organisms depending on its concentration and speciation in solution. Human activities mobilize and spread large quantities of zinc broadly in the environment. Discriminating the natural and various anthropogenic zinc sources in the environment and understanding zinc's fate at a catchment scale are key challenges in preserving the environment. This review presents the state of the art in zinc isotope studies applied to environmental purposes at a river-basin scale. Even though the study of zinc isotopes remains less developed than more “traditional” lead isotopes, we can assess their potential for being a relevant tracer of zinc in the environment. We present the principles of zinc isotope measurements from collecting samples to mass spectrometry analysis. To understand the fate of zinc released in the environment by anthropogenic activities, we summarize the main processes governing zinc distribution between the dissolved and solid phases, with a focus on the isotope fractionation effects that can modify the initial signature of the various zinc sources. The signatures of zinc isotopes are defined for the main natural sources of zinc in the environment: bulk silicate earth (BSE), zinc sulfide ore deposits, and coal signatures. Rivers draining natural environments define the “geological background for surface water”, which is close to the BSE value. We present the main anthropogenic sources (metallurgical waste, effluents, fertilizers, etc.) with their respective isotope signatures and the main processes leading to these specific isotope characteristics. We discuss the impact of the various anthropogenic zinc

emissions based on the available studies based on zinc isotopes. This literature review points out current knowledge gaps and proposes future directions to make zinc isotopes a relevant tracer of zinc (and associated trace metals) sources and fate at a catchment scale.

Keywords

Zinc isotopes, metals, contamination, source tracer, catchment.

1. Introduction

Zinc (Zn) is ubiquitous, being present in soils, plants and biota, acting both as an essential and a toxic element to organisms depending on its concentration and speciation in solution (e.g. Campbell, 1995; Whitton, 1970). For instance, zinc depletion produces nutrient limitation in the sea, whereas excess zinc can cause a range of reproductive, developmental, behavioral, and toxic responses in a variety of aquatic organisms and insects (e.g. Muyssen et al., 2006; Schmidt et al., 2011). Concerning human health, a surplus of zinc is associated with oxidative stress and is a contributing factor in many chronic diseases (e.g. Walsh et al., 1994). Many human activities make and mobilize widespread large quantities of zinc in the environment. Industries and wastewater treatment plants expel their zinc-rich liquid effluents directly into rivers. Emissions from metal processing (mining and smelting) are a major source of zinc in the atmosphere and soil (Nriagu and Pacyna, 1988). Coating steel by “hot dip” galvanization or zinc electroplating (also called “electrogalvanization”) is a common use of zinc, and zinc in these products may be easily released into the environment through corrosion. Other sources of zinc contamination include the disposal of fertilizers and crop protection treatments in cultivated areas (Eriksson, 2001). Zinc is also transferred to the atmosphere and soil through coal combustion and waste incineration (Abanades et al., 2002; Xu et al., 2004). Non-combustion traffic emissions relative to vehicles (tires and brakes) and road furniture (galvanized parts and railings) also spread this metal into the environment (Councell et al., 2004; Legret and Pagotto, 1999; Zarcinas and Rogers, 2002). These various zinc contributions, deposited in the environment in particulate form or in larger deposits, are leached by rainfall, forming water runoff with high Zn concentrations. These releases then join rivers, polluting riverbed sediments and the water itself. River basins play a key role in the water cycle, capturing and storing enormous quantities of water, which ultimately supply a large part of the available freshwater on Earth. Thus, controlling Zn concentrations in surface water is a major environmental and public health issue.

The European Union (EU) Water Framework Directive (2000/60/EC) aims to deliver integrated river basin management for the whole of Europe. The member states of the EU are required to prepare a list of specific pollutants and their environmental quality standards (EQS) in the aquatic environment for evaluating the ecological status of water. Metal zinc, regulated by 22 EU member states, is the river basin-specific pollutant most often monitored in the EU (Arle et al., 2016). The predicted no-effect concentration (PNEC) from the EU Risk Assessment Reports varies depending on the water hardness, with the lowest EQS at 7.8 µg/L (Kos Durjava et al., 2015). In France, an acceptable ecological status for a water body is reached, without a hardness condition, when the bioaccessible zinc content is below 7.8 µg/L (Statute of 27 July 2015, https://substances.ineris.fr/fr/page/9). In the USA, the water quality criterion recommended by the United States Environmental Protection Agency, below which significant risks to the majority of species in a given environment are not expected, is 66.6 µg/L at a hardness of 50 mg/L (United States Environmental Protection Agency, 1996). For good management of water bodies, defining numerical limits for zinc in the environment below which unacceptable effects are not expected is not enough. Indeed, the multiplicity of pollution sources, the presence of variable “naturally” occurring background concentrations, the existence of a number of chemical species with various toxicity, and how the abundance of those species changes in response to changes of the water’s physical and chemical conditions must be considered.

Within the last twenty years, developments in mass spectrometry (TIMS, thermal ionization mass spectrometry and MC-ICP-MS, multicollector-inductively coupled plasma-mass spectrometry) have allowed the high-precision measurement of isotope compositions of transition metals and post-transition metals such as zinc (e.g. Maréchal et al., 1999; Schoenberg and Von Blanckenburg, 2005; Schönbächler et al., 2007). Zinc has five stable isotopes, ^{64}Zn, ^{66}Zn, ^{67}Zn, ^{68}Zn, and ^{70}Zn, with natural abundances of 49.2, 27.8, 4.0, 18.4, and 0.6% respectively. Since the pioneering work of Maréchal et al. (1999), the application of Zn isotope biogeochemistry has rapidly expanded, and Zn isotope compositions have been

used in various domains and already discussed in review papers (Albarède, 2004; Cloquet et al., 2008; Moynier et al., 2017; Yin et al., 2015). This review is specifically dedicated to the use of Zn isotopes as tracers to determine the sources of anthropogenic pollution and how they were transported into rivers. This review compiles and discusses currently available data from these previous studies, together with unpublished data from the Loire River Basin (France). From this compilation we have evaluated the ability of Zn isotope compositions to trace metal sources at the catchment scale, in both dissolved and solid phases.

2. Materials and methods

The mass of zinc typically required for mass spectrometry analysis (at least 4 replicates) is 1 µg (e.g. Chen et al., 2009a; Guinoiseau et al., 2017). Several steps (i.e. collection, preparation and measurement) are necessary to acquire the isotope composition of natural sample. Because metals are everywhere in field and laboratory equipment, costly and time-consuming procedures are required to minimize zinc contaminations during these steps. All reagents are prepared with 18.2 MΩ.cm (at 25 °C) water and commercial acid purified in laboratory by sub-boiling distillation (e.g. Araújo et al., 2017a; Bermin et al., 2006). All materials, including PFA vessels, pipette tips, columns, and bottles, are previously cleaned in a laboratory with nitric and/or hydrochloric acid and then rinsed thoroughly with 18.2 MΩ.cm water prior to use (e.g. Balistrieri et al., 2008; Bryan et al., 2015). According to previous studies (Bryan et al., 2015; Nelson et al., 2017), polyvinyl gloves, which are commonly manufactured using zinc stearate as a mold release compound, must not be used when handling samples and hardware. Total procedural blanks (from field to mass spectrometry analysis) must be regularly measured to verify the cleaning procedure. Procedural blanks are generally lower than 10 ng, which represented less than 1% of the mass of zinc analyzed (e.g. Chen et al., 2009a; Guinoiseau et al., 2017).

2.1 Sampling requirements for zinc isotope analyses in water and sediments

We have seen that all materials used in the field to collect samples must be previously cleaned in the laboratory. To determine Zn isotope compositions in solution in liquid samples (surface water, effluent, etc.) the sample volume taken in the field varies between a few tens of milliliters to several liters according to the concentration of the medium. Samples are taken using plastic containers, then generally filtered at 0.20 µm or 0.45 µm and placed in plastic bottles rinsed several times with water filtered from the sample (e.g. Aranda et al., 2012; Borrok et al., 2008; Chen et al., 2008; Petit et al., 2015; Szynkiewicz and Borrok, 2016; Wanty et al., 2013). Water samples are preserved with sub-boiled concentrated nitric or hydrochloric acid to a pH of approximately 2 (e.g. Aranda et al., 2012; Chen et al., 2014).
Recently, passive diffusive gradients in thin film samplers (DGT samplers) have been also used successfully for Zn isotope measurements in surface water (Desaulty et al., 2017; Desaulty and Millot, 2017). DGT can pre-concentrate metals in situ and provide an isotope composition of water integrated over time.

For solid samples, the quantity of materials sampled is not governed by the concentration of solid metals (generally a few hundred mg/kg), which is high compared with the quantity necessary for isotope analysis (1 µg of Zn), but usually considers the need for representative samples. Stream sediments are sampled from the middle of water courses with sampling media (shovels, augers, etc.) not containing zinc and not coated with painted surfaces that contain metal-based pigments (Bullen, 2012). The sediment cores are generally taken using acrylic tubes (Araújo et al., 2017a; Sivry et al., 2008). To obtain the required mass of suspended particulate matter (SPM) for isotope and chemical analyses (>50 mg) a large volume of water is collected (often more than 1 L) and then filtered or centrifuged to recover all SPM (Araújo et al., 2017b; Chen et al., 2009b; Guinoiseau et al., 2017; Petit et al., 2015, 2008).

2.2 Chemical separation and analysis of zinc isotopes

Prior to isotope analyses, preparation (e.g. solid dissolution) and chemical purification are necessary to separate zinc from coexisting matrix elements. Sample preparation takes place in a cleanroom under positive pressure of filtered air, under a laminar airflow, allowing all phases of sample preparation to be performed under clean conditions (e.g. Borrok et al., 2008; Petit et al., 2015). The chemical purification is generally performed with anion-exchange chromatography in concentrated HCl on macro-porous, pre-cleaned resin (AG-MP1, BioRad®) (e.g. Borrok et al., 2007; Maréchal et al., 1999).

While Zn isotope compositions were initially measured by TIMS (Thermal-ionization mass spectrometry) (Rosman, 1972), it is high-precision measurement by MC-ICP-MS (Maréchal et al. (1999)) that led to the rapid expansion of Zn isotopes into a variety of environmental applications. Several methods are used for correcting isotope discrimination in the instrument during analysis. Zn isotope data can be acquired by MC-ICP-MS, either by standard-sample bracketing or by the double-spike method. Standard-sample bracketing involves analyzing a standard solution directly before and after a sample. This method is often associated with external normalization, which consists, prior to the analysis, of adding to the sample another element having an atomic mass close to that of the element of interest. Zinc data are generally externally normalized to copper (Cu) using an exponential mass-fractionation law (Archer and Vance, 2004; Maréchal et al., 1999). Standard-sample bracketing needs complete recovery of the element during chemical preparation to avoid mass discrimination leading to analysis that would not be representative of the bulk sample. In the double-spike method, before chemical preparation, a mixture of two isotopes of the element (generally ^{64}Zn-^{67}Zn) with a non-natural isotopic composition are added (Arnold et al., 2010a; Bermin et al., 2006). The advantage of using a double-spike method is that the complete recovery of the element during chemical preparation is not necessary. Moreover, since the mass bias is corrected using an isotope ratio of the analyte element, this method is little affected by matrix-induced mass bias effects. The double-spike method is particularly well adapted for samples

that only contain small amounts of zinc (a few µg/L) in a matrix with much higher concentrations of other elements such as seawater and biological materials (e.g. Arnold et al., 2015; Zhao et al., 2014). In spite of the advantages of the double-spike method, due to its straightforward approach the standard-sample bracketing method is still in widespread use in recent MC-ICP-MS Zn isotope studies (e.g. Araújo et al., 2019; Gelly et al., 2019).

Zn isotope compositions are reported as a classical δ-notation (parts per thousand, ‰) with the $^{66}Zn/^{64}Zn$ ratio relative to zinc standard:

$$\delta^{66/64}Zn\,(‰) = \left[\frac{(^{66}Zn/^{64}Zn)_{sample}}{(^{66}Zn/^{64}Zn)_{standard}} - 1\right] \times 1000$$

After the standard used in the original work by Maréchal et al. (1999) i.e. JMC 3-0749C (usually called JMC-Lyon) a number of different reference standards have been developed and used in a routine manner in different laboratories (SRM NIST 683, IMC 12053, PCIGR-1, IRMM-3702, Imperial) (e.g. Moeller et al., 2012; Yang et al., 2018). Despite JMC-Lyon having not been available for many years, data are generally normalized to this standard. All data presented in this review were recalculated referring to JMC-Lyon for easy comparison.

The precision of Zn isotopic measurements depends on the quality of the chemical preparation (total procedural blanks relative to content in sample, quantitative recovery of the element) and on the operating parameters and corrections applied during MC-ICP-MS measures. In recent studies, typical analytical precision for $\delta^{66/64}Zn$ measurements verified by repeated runs of samples and standards is generally around ± 0.05‰ (2σ) for environmental samples regardless of the method used to correct the instrumental bias (e.g. Araújo et al., 2019; Vance et al., 2016) .

2.3 Additional data from the Loire River Basin

The corpus of samples coming from the Loire River Basin was composed of liquid and solid samples described in supplementary Tables S1, S2, and S3. Liquid effluents coming from various industries and wastewater treatment plants (WWTP) that are usually directly discharged into the Loire river were analyzed (Table S1). Other samples containing high Zn contents were also analyzed (organic fertilizers and brake pads) (Table S1). Pig slurry and manure samples were sampled in Brittany and Pays de la Loire (France) and brake pad linings commercially available in France were purchased (Valeo®). Dissolved loads were sampled from the Loire River Basin in an upstream/downstream transect, as well as the Furan River draining various sulfide mineralizations (Table S2). SPM was collected in the Loire River before the estuary (Montjean-sur-Loire) (Table S3). SPM and sediments were collected in the watershed mainly occupied by intensive farming (Argos, Vilaine, Couesnon) (AELB, 2013) (Table S3). The sampling and analysis protocols were in line with these described above (sections 2.1. and 2.2.) and detailed in supplementary materials.

3. Impact of natural physical and chemical processes on zinc isotope compositions

Various processes control metal distribution between the dissolved and particulate phases in surface water. The main mechanisms causing a new Zn isotope distribution between the phases (i.e. isotope fractionation) are equilibrium isotope distribution between dissolved aqueous species and equilibrium and kinetic effects due to the interactions between minerals or live organisms and aqueous solutions (adsorption, precipitation, uptake, etc.). The goal of this article is not to make an exhaustive study of the fractionation that affects Zn isotope compositions in the environment, but to highlight the main processes that govern zinc distribution between dissolved and particulate phases and to evaluate how they affect the initial $\delta^{66/64}$Zn signatures of anthropogenic zinc sources. Isotope fractionation between zinc bound, fixed or adsorbed on a solid organic or inorganic phase and zinc in solution is defined as follows:

220 $$\Delta^{66/64}Zn_{solid\text{-}dissolved}=\delta^{66/64}Zn_{solid}-\delta^{66/64}Zn_{dissolved}$$

221 Laboratory experimental studies investigated the mechanisms that potentially fractionate Zn
222 isotopes (Fernandez and Borrok, 2009; Guinoiseau et al., 2016; Veeramani et al., 2015).
223 These various mechanisms (adsorption, dissolution, precipitation etc.) and their impact on
224 isotope signatures as described in the literature are summarized in Fig. 1. These
225 experiments can be also coupled with X-ray absorption spectroscopy, which provides the
226 metal's local structural information (i.e., coordination number, bond distance) allowing to
227 make the link between changes in crystal-chemical parameters and the isotope
228 fractionations. This technique is mainly used to study the chemical environment of zinc
229 during adsorption onto several minerals (Gou et al., 2018; Juillot et al., 2008; Nelson et al.,
230 2017).

231 Several theoretical studies used *ab initio* and density functional methods to determine
232 equilibrium stable isotope partitioning between various zinc species by calculating their
233 reduced partition function ratios (RPFR or β). The fractionation between two species A and B
234 is then defined as the ratio of their β-factors $\alpha^{66/64}{}_{A\text{-}B}=\beta^{66/64}{}_{A}/\beta^{66/64}{}_{B}$ and a simple relation
235 allows the comparison of these theoretical equilibrium isotopic fractionations and $\delta^{66/64}Zn$
236 values, which are commonly reported on natural samples:

237 $$10^3 \ln \alpha^{66/64}{}_{A\text{-}B} \sim \Delta^{66/64}Zn_{A\text{-}B} = \delta^{66/64}Zn_A - \delta^{66/64}Zn_B$$

238 By calculating β-factors we identify some of the crystal-chemical parameters controlling
239 isotopic properties. In particular, the proprieties of bonds between zinc and its neighbors is
240 an important crystal-chemical parameter controlling isotopic fractionation between phases.
241 General theoretical considerations suggest that the lower coordination states and bond
242 lengths should prefer the heavy isotope (Schauble, 2004). Equilibrium stable isotope
243 partitioning between aqueous zinc complexes including aqueous sulfate, chloride, and
244 carbonate species are determined by previous studies (Black et al., 2011; Fujii et al., 2014,
245 2011, 2010). Zinc complexes (Zn phosphates, citrates and malates) were also modeled to

discuss the Zn isotope fractionation in roots and leaves of plants (Fujii and Albarède, 2012). In their review study, Moynier et al. (2017) summarized the calculated β-factors available in the literature for aqueous solutions and molecules relevant for zinc in biogeochemistry. Their study also provides unpublished data for various molecules (e.g. oxalate species). Ducher et al. (2018, 2016) used also *ab initio* calculations to determine equilibrium Zn isotope fractionation factors in Zn-bearing minerals (e.g. sphalerite, hydrozincite) and between hexaaquo zinc complexes and minerals. Although a straightforward comparison between the various theoretical data available in the literature is difficult since the β-factors have been determined with different types of input data and methods (Black et al., 2011; Ducher et al., 2016; Fujii et al., 2010), these data provide a theoretical basis for the interpretation of Zn isotopic measurements. The β-factors for various dissolved species, organic ligands, Zn-bearing minerals and zinc metal are represented in supplementary Fig. S1 (Black et al., 2011; Ducher et al., 2018, 2016; Fujii et al., 2014; Fujii and Albarède, 2012; Moynier et al., 2017). To compare the β-factors and evaluate the isotope fractionation between phases, in this publication we considered an ambient temperature of 25°C.

Distribution between dissolved aqueous species. In aqueous solutions, stable Zn complexes depend on the dominant ligands (Albarède, 2004). At increasing chlorine and sulfate concentrations, the hexaaquo zinc complex $Zn(H_2O)_6^{2+}$ gives zinc-chloro complexes (e.g. $ZnCl(H_2O)_5)^+$, $ZnCl_2(H_2O)_4$) and zinc-sulphato complexes (e.g. $ZnSO_4(H_2O)_6$, $ZnSO_4(H_2O)_5$). *Ab initio* calculations showed that aquo-ion and zinc chloride complexes have close isotope signatures (Fujii et al., 2014), whereas zinc sulfates are enriched in ^{66}Zn with a value of $\Delta^{66/64}Zn$ ~+0.5‰ relative to aquo-ions (Moynier et al., 2017) (Fig. S1). With increasing pH, carbonate ($ZnCO_3(H_2O)_3$) and hydroxide ($Zn(OH)_2(H_2O)_4$) become the dominant species with $\Delta^{66/64}Zn$ enrichment until +1‰ for zinc carbonates relative to aqua-ion (Fujii et al., 2014).

Organic complexation. A major part of “dissolved” zinc in rivers is organically complexed rather than free and inorganically complexed; this part of organically complexed Zn increases

greatly in estuary zones (e.g. Montgomery and Santiago, 1978; van den Berg and Dharmvanij, 1984). Experiments dedicated to complexation on organic compounds' humic acid (an organic matter analog) showed that below pH 6 isotope fractionation is not measurable, while at higher pH the complexed organic Zn is heavier than free Zn^{2+} ($\Delta^{66/64}Zn$ =+0.24‰) (Jouvin et al., 2009). The authors explained this difference by changes in Zn speciation with pH, with higher complexation constants and shorter bond lengths for organic complexed Zn compared to the free Zn^{2+}. Ban et al. (2002) measured similar fractionation ($\Delta^{66/64}Zn$= +0.20‰) between EDTA complexed Zn and Zn^{2+}. Theoretical equilibrium isotopic factors seem to confirm these experimental results. β-factor for citrate, another analog for humic acids, showed that the predominant species present in solutions at pH between 4 and 8, $Zn(cit)(H_2O)_3^-$, is enriched in ^{66}Zn compared to the hexaaquo zinc complex with $\Delta^{66/64}Zn$=+0.16‰ (Fujii et al., 2014; Fujii and Albarède, 2012) (Fig. S1).

Adsorption onto mineral particles. Adsorption of zinc onto mineral particles (oxides, oxide-hydroxides, clay, carbonate and silicates) causes a drop in the $\delta^{66/64}Zn_{dissolved}$ value with $\Delta^{66/64}Zn$ fractionation around +0.30‰. This depends on the nature of the mineral and the solution conditions (pH, ionic strength) (Balistrieri et al., 2008; Bryan et al., 2015; Dong and Wasylenki, 2016; Gou et al., 2018; Guinoiseau et al., 2016; Juillot et al., 2008; Nelson et al., 2017; Pokrovsky et al., 2005). In most cases, the fractionation is driven by a decrease of coordination number and bond lengths between aqueous Zn (six-coordinate octahedral) and adsorbed Zn (four-coordinate tetrahedral) complexes.

Precipitation. While synthetic hydrozincites ($Zn_5(CO_3)_2(OH)_6$) produced by Wanty et al., 2013 have $\delta^{66/64}Zn$ identical to the dissolved Zn, Veeramani et al. (2015) showed that hydrozincite and hopeite ($Zn_3(PO_4)_2.4H_2O$) precipitation tends to reduce the $\delta^{66/64}Zn_{dissolved}$ value ($\Delta^{66/64}Zn$ = +0.18‰ and +0.25‰ respectively). The $\delta^{66/64}Zn_{dissolved}$ value in a river draining a Zn-Pb mining district in Sardinia and containing a consortium of a microalga and a cyanobacterium, which facilities the biomineralization of hydrozincite, is also significantly

depleted in heavy isotopes compared to hydrozincite ($\Delta^{66/64}$Zn= +0.35‰) (Wanty et al., 2013). Data obtained by Veeramani et al. (2015) (and also Wanty et al. (2013) for natural samples) are in agreement with the theoretical fractionation value calculated by Ducher et al. (2018) between hydrozincite precipitate and hexaaquo zinc complex ($\Delta^{66/64}$Zn ~ +0.30‰, Fig. S1).

Laboratory experiments with and without bacteria showed that sphalerite (ZnS) precipitation increases $\delta^{66/64}Zn_{dissolved}$ relative to the precipitate ($\Delta^{66/64}$Zn fractionation of -0.30‰) (Archer et al., 2004; Jamieson-Hanes et al., 2017; Veeramani et al., 2015). This isotope fractionation is consistent with *ab initio* calculations that predict a fractionation of -0.50‰ between sphalerite precipitate and hexaaquo zinc complex (Ducher et al., 2018) (Fig. S1).

Dissolution. Using the same calculation, sphalerite dissolution should lead to fractionation between solid and aqueous Zn of $\Delta^{66/64}$Zn ~ -0.50‰, whereas during oxidative weathering experiments of sphalerite-rich rocks Fernandez and Borrok (2009) measured only a little initial fractionation ($\Delta^{66/64}$Zn = -0.20‰) that quickly dissipated to give a $\delta^{66/64}Zn_{dissolved}$ close to sphalerite ($\Delta^{66/64}$Zn = 0.0‰). The initial fractionation can be explained by the transient formation of a surface coating on sphalerite composed of Zn sulfates (Fernandez and Borrok, 2009). The theoretical β–factor for Gunningite ($ZnSO_4$. H_2O) showed that this phase preferentially incorporates the heavier Zn isotopes compared to sphalerite ($\Delta^{66/64}$Zn ~ +0.30‰) and is weakly deleted in heavy isotope compared to Zn^{2+} ($\Delta^{66/64}$Zn ~ -0.20‰, Ducher et al., 2018) (Fig. S1).

According to the β-factor values, the dissolution of metallic zinc leads to an enrichment in ^{66}Zn for hexaaquo zinc complex with $\Delta^{66/64}$Zn ~ -1.5‰ (Black et al., 2011) (Fig. S1).

Adsorption onto biological surfaces. Adsorption of zinc onto microorganisms (bacteria, diatoms, plankton, phototrophic biofilm) generally increases the $\delta^{66/64}Zn_{adsorbed}$ value with $\Delta^{66/64}$Zn fractionation between +0.30 and +1.20‰ that depends on the nature of microorganisms and the solution conditions (pH, ionic strength) (Coutaud et al., 2014;

Gélabert et al., 2006; John and Conway, 2014; Kafantaris and Borrok, 2014). In most cases, the fractionation seems driven by a mechanism similar to a Zn complexation to organic functional groups on organisms' external surfaces.

Biological uptake. The uptake by plants (rice, tomato, etc.) and microorganisms (diatom, bacteria, plankton, phytoplankton) may increase or decrease the $\delta^{66/64}Zn_{dissolved}$ value according the uptake process involved (high or low affinity pathway), which depends on the concentration of free ions in the nutrient solution (Arnold et al., 2015, 2010b; Aucour et al., 2015, 2011; Caldelas et al., 2011; Couder et al., 2015; Coutaud et al., 2014; Gélabert et al., 2006; Houben et al., 2014; John et al., 2007a; Jouvin et al., 2012; Kafantaris and Borrok, 2014; Samanta et al., 2018; Smolders et al., 2013; Tang et al., 2016; Viers et al., 2007; Weiss et al., 2005). The uptake of heavy isotopes by microorganisms and plants is favored in low Zn concentration media (~1-10 µg/L). The mechanism is the active uptake by a membrane transport protein Zn-ion-permease or by a chelating organic complex Zn-phytosiderophore (high affinity uptake) (e.g. Arnold et al., 2010b; Tang et al., 2016). Microorganisms and plants preferentially take up the lighter isotopes of zinc when the mechanism is diffusive transport across the cell membrane and through the boundary layer of the root (low affinity uptake) (e.g. John et al., 2007a; Jouvin et al., 2012). For plants, we do generally see a higher $\delta^{66/64}Zn$ value in roots than in the nutrient medium with a preferential translocation of light isotopes into the upper parts (Fig. 3). Fujii and Albarède (2012) explained these results using *ab initio* calculations and proposed that the fractionation is driven by the difference in Zn speciation between the root system (isotopically heavy Zn phosphates) and the upper parts, rich in isotopically light citrates and malates (Fig. S1).

4. Isotope composition of natural zinc sources

4.1 The Upper Continental Crust

The average Zn content in the upper continental crust calculated by Taylor and McLennan (1985) is 71 mg/kg. For rocks in the continental crust, analysis of Zn isotope compositions ($\delta^{66/64}Zn$) in granite shows values between +0.21 and +0.47‰ (n=4, Araújo et al., 2017a; Chen et al., 2009b; Chen et al., 2016; Viers et al., 2007). Based on basaltic and ultramafic sample analyses from different geologic settings, Chen et al. (2013) estimated the average Zn isotope composition of bulk silicate earth (BSE) to be $\delta^{66/64}Zn = +0.28 \pm 0.05‰$ (2σ).

4.2 Sulfide and non-sulfide ore deposits

The main zinc ore exploited is sphalerite or blende (ZnS). It represents 90% of current world zinc production (Gordon et al., 2003); various zinc minerals such as smithsonite ($ZnCO_3$) also called calamine, account for the rest (Gordon et al., 2003). Since zinc is present in ores in only a single oxidation state (+II), the variety of isotope compositions in the various mineralizations is limited compared to other metal elements like copper (between -3 and +7‰ e.g. Braxton and Mathur, 2011; Maréchal et al., 1999) (Fig. 2). However, the fact that zinc is in various crystallographic environments and coordination numbers (ranging from 4 to 6) in Zn-bearing minerals lead to a significant theoretical fractionation between ores until $\Delta^{66/64}Zn \sim +1.5‰$ (Ducher et al., 2016) (Fig. S1). For silicate and carbonate minerals, in accordance with the general rule of short bonds concentrating heavy isotopes (Schauble, 2004), a general decrease in β-factors is observed when the bond lengths and coordination numbers increase (Ducher et al., 2016). The highest β-factor value is found for hemimorphite ($Zn_4Si_2O_7(OH)_2.H_2O$) where Zn atoms are four-fold coordinate with O atoms. The β-factor for willemite (Zn_2SiO_4) is not calculated by Ducher et al. (2016). However, Zn being tetrahedrally coordinated with oxygen in willemite like in hemimorphite, it is likely that the β-factors for these phases would be comparable (Mondillo et al., 2018). In hydrozincite ($Zn_5(CO_3)_2(OH)_6$) the β-factor is lower relative to hemimorphite due to the fact that Zn is found in both tetrahedral and octahedral sites. Smithsonite where Zn is octahedrally coordinated have the lowest β-factor. With β-factor close to smithsonite and Zn tetrahedrally coordinated,

376 sphalerite is out of this general trend because Zn-S bond properties differ from Zn-O bonds
377 (Fig. S1).

378 For sphalerite and other sulfur-containing minerals like galena (PbS) and chalcopyrite
379 ($CuFeS_2$) sampled worldwide, the Zn isotope variations ($\delta^{66/64}Zn$) are relatively low with an
380 interquartile range (IQR) of between +0.05 and +0.26‰ and a mean and median of +0.16‰
381 (n = 294) (Aranda et al., 2012; Chapman et al., 2006; Deng et al., 2017; Duan et al., 2016;
382 Gagnevin et al., 2012; John et al., 2008; Kelley et al., 2009; Maréchal et al., 1999; Mason et
383 al., 2005; Mattielli et al., 2009; Mondillo et al., 2018; Novak et al., 2016; Pašava et al., 2014;
384 Shiel et al., 2010; Sivry et al., 2008; Skierszkan et al., 2016; Sonke et al., 2008; Voldrichova
385 et al., 2014; Wanty et al., 2013; Weiss et al., 2007; Wilkinson et al., 2005; Zhou et al., 2014)
386 (Fig. 2; supplementary Fig. S2). The variability of $\delta^{66/64}Zn$ signatures for sphalerite within a
387 deposit is likely due to a kinetic fractionation and Rayleigh distillation during progressive
388 sphalerite precipitation from hydrothermal fluids (Wilkinson et al., 2005). Theory predicts that
389 kinetically controlled reactions favor the incorporation of isotopically light zinc in mineral
390 precipitates relative to the bulk ore-forming fluid (Wilkinson et al., 2005), which likely explains
391 the mean and median value for $\delta^{66/64}Zn$ values in sulfide ore deposits, depleted in heavy
392 isotopes compared to the BSE value (+0.28 ± 0.05‰, 2σ).

393 Secondary minerals, such as willemite, smithsonite, hydrozincite, and hemimorphite, formed
394 through low-temperature hydrothermal and/or supergene oxidation of primary sulfide
395 deposits, have more variable Zn isotope compositions than primary sulfide ores with $\delta^{66/64}Zn$
396 values generally between +0.05 and +0.48‰ and a median value of +0.28‰ (n = 23, IQR)
397 (Araújo et al., 2017a; Mondillo et al., 2018; Pašava et al., 2014; Voldrichova et al., 2014)
398 (Fig. 2; Fig. S2). These minerals form through the total or partial release of zinc by
399 dissolution from a precursor phase (primary sphalerite or an earlier secondary phase). The
400 complete breakdown of primary sulfides/minerals and quantitative reprecipitation of zinc
401 leads to low fractionation, whereas partial dissolution and incorporation causes high
402 fractionation between phases. Pašava et al. (2014) studied Zn isotope composition in

minerals at La Florida mine (Spain), where an intense supergene alteration of sphalerite leads to the formation of secondary minerals like hydrozincite that are significantly enriched in heavy isotopes relative to sphalerite ($\Delta^{66/64}$Zn = +0.60‰). For ores coming from the Czech Republic, Voldrichova et al. (2014) showed a strong enrichment in heavy isotopes for hemimorphite relative to sphalerite ($\Delta^{66/64}$Zn = +0.80‰). These fractionations are consistent with β-factors calculated between hydrozincite, hemimorphite and aqueous Zn by Ducher et al. (2018) ($\Delta^{66/64}$Zn=+0.30‰ and $\Delta^{66/64}$Zn=+0.90‰ respectively). Mondillo et al. (2018) studied Zn isotope compositions in secondary zinc minerals collected from Zn deposits in Ireland, Belgium, Poland, Namibia, and Zambia, formed during low-temperature hydrothermal and/or supergene oxidation of primary sulfide deposits. Most of the data observed on minerals can be explained as described above by an isotopic fractionation model in which the partial dissolution of primary sphalerite is followed by the precipitation of an initial secondary phase that preferentially incorporates light Zn isotopes (smithsonite) or heavy Zn isotopes (hemimorphite, willemite, hydrozincite) (Fig. S1). However, Mondillo et al (2018) observed also strong negative isotopic shifts for late crystallizing phases ($\Delta^{66/64}$Zn = -0.50‰ for Willemite and $\Delta^{66/64}$Zn=-0.66‰ for hemimorphite relative to a precursor phase). Authors explained these low Zn isotope signatures for late crystallizing phases relative to the precursor mineral by the progressive precipitations from fluids that form phases enriched in heavy Zn isotopes leading to a gradual decrease in the $\delta^{66/64}$Zn values of such phases, and the fluids involved, in time and space. In conclusion, the variability of $\delta^{66/64}$Zn values in secondary ores (between +0.05 and +0.48‰, n = 23, IQR), higher than for primary sulfides (between +0.05 and +0.26‰, n = 294, IQR), can be explained by a combination of equilibrium isotope fractionation and open system Rayleigh distillation during incomplete dissolution–reprecipitation reactions.

4.3 Coal

In coal, the Zn content can reach several hundreds of mg/kg (Novak et al., 2016). Zn isotope compositions in coal vary very widely with $\delta^{66/64}$Zn values generally between -0.10 and +1.35‰ (n = 14, IRQ) for samples taken in Spain, the Czech Republic, Germany and the USA (Borrok et al., 2010; Novak et al., 2016; Ochoa Gonzalez and Weiss, 2015; Voldrichova et al., 2014) (Fig. S2). The wide variability of coal isotope compositions is related to diagenetic processes (uptake by plants, exchange with pore waters) that occur in peat, a coal precursor (Ochoa Gonzalez and Weiss, 2015).

4.4 Natural water

In rivers that are largely unaffected by human activity, Zn concentrations in solution (dissolved load) are generally between 1 and 2 µg/L (Gaillardet et al., 2003). For rivers with little human impact, the Zn concentrations in solution are substantially lower than the European (7.8 µg/L) and US (66.6 µg/L) EQS values. The particulate phase (sediment & SPM) in rivers generally contains higher quantities of zinc, at around 200 mg/kg for rivers with little human impact (Martin and Meybeck, 1979; Viers et al., 2009). In waters with little human impact ($[Zn]_{dissolved} \leq 2$ µg/L), the isotope compositions of Zn in solution are generally between $\delta^{66/64}$Zn = +0.29 and +0.57‰ (n=63, IQR) (Chen et al., 2014, 2008; Little et al., 2014; Petit et al., 2015; this study) (Fig. S2). However, we note great variability in $\delta^{66/64}$Zn values in estuaries. A study on the Garonne estuary (France) showed that in the turbidity zone the dissolved $\delta^{66/64}$Zn values varied from +0.19 to +0.90‰ from upstream to downstream unlike $\delta^{66/64}$Zn in SPM, which remained constant (+0.37 ± 0.05‰, 2σ, n=10) (Petit et al., 2015) (Fig. 3). Although not consistent with fractionation experiments at isotopic equilibrium (Fig. 1), the authors explained this enrichment by kinetically driven adsorption due to strongly increasing sorption sites in the turbidity zone (Petit et al., 2015). The $\delta^{66/64}$Zn values for zinc in solution in the estuary of the river Kalix (Sweden) and the Amazon estuary (Brazil), between +0.36 and +0.80‰ (n = 7, Little et al., 2014), are also high compared to the BSE level (+0.28 ± 0.05‰, 2σ) (Fig. 3). As shown previously (see section 3) the part of

454 “dissolved” Zn complexed to organic ligands relative to free and inorganically complexed Zn
455 increases widely in estuaries compared to upstream. The organic complexed Zn enriched in
456 ^{66}Zn compared to the free Zn^{2+} (Fig. 1), could participate in the enrichment in heavy isotopes
457 of dissolved Zn in the estuary zone compared to upstream. At the river–sea interface, in
458 addition to physical and chemical processes, mixing between fresh water and seawater
459 ($\delta^{66/64}Zn$ ~ +0.50‰; Boyle et al., 2012; Zhao et al., 2014) may also explain part of the
460 variability observed. If we do not consider estuaries, the variation in $\delta^{66/64}Zn$ in solution in
461 rivers with little human impact ($[Zn]_{dissolved}$ ≤ 2 µg/L) is quite small, with values between +0.28
462 and +0.43‰ (n=46, IQR) and a median value of +0.33‰ close to the BSE value (+0.28 ±
463 0.05‰, 2σ) (Fig. 3). Most of the sediments and SPM taken from lakes and rivers with little
464 human impact ($[Zn]_{particulate}$ ≤ 200 mg/kg) have Zn isotope compositions varying from
465 $\delta^{66/64}Zn$=+0.14 to +0.32‰ (n= 129, IQR, Araújo et al., 2017a, 2017b, 2019, 2018; Chen et al.,
466 2009b; Guinoiseau et al., 2018, 2017; Petit et al., 2015, 2008; Sivry et al., 2008; Thapalia et
467 al., 2010, 2015; this study) (Fig. S2). SPM generally has isotope compositions similar to or
468 slightly lower than the associated dissolved phase (Chen et al., 2009b, 2008). This result
469 suggests that adsorption processes are not the dominant process by which Zn enrichment in
470 SPM occurs (Chen et al., 2009b), and that the organic matter in both the sediment and
471 aqueous phase likely plays a crucial role in the distribution of Zn isotopes between these
472 phases. In Fig. 3 where $\delta^{66/64}Zn$ values are shown for sediments and SPM of lakes and rivers
473 with little human impact ($[Zn]_{particulate}$ ≤ 200 mg/kg) we see that the Amazon and its tributaries,
474 including the Rio Negro, have a considerably lower isotope signature (+0.07 ± 0.30‰, 2σ, n
475 = 48) compared to the BSE value (+0.28 ± 0.05‰, 2σ). This specific isotope composition is
476 related to the presence in Rio Negro SPM of kaolinite in which zinc is structurally
477 incorporated (Guinoiseau et al., 2018). If we do not consider this watershed, Zn isotope
478 compositions in SPM and sediments for lakes and rivers with little human impact ($[Zn]_{particulate}$
479 ≤ 200 mg/kg) have quite a narrow variation with values between +0.23 and +0.40‰ (n=81,
480 IQR) and a median value of +0.30‰, similar to the BSE value (+0.28 ± 0.05‰, 2σ) (Fig. 3).

These data on $\delta^{66/64}$Zn values in the dissolved phase (between +0.28 and +0.43‰, n=46, IQR) and the particulate phase (between +0.23 and +0.40‰, n=81, IQR) for lakes and rivers let us define a composition for the geological background for surface water (GBSW) with values between +0.24 and +0.41‰ (n=127, IQR) and a median value +0.30‰, similar to the BSE value (+0.28 ± 0.05‰, 2σ) (Fig. S2).

5. Isotope composition of anthropogenic zinc sources

Considerable quantities of zinc are emitted into the environment by industry, urbanization and agriculture. A summary of major anthropogenic zinc flows emitted into the environment in France is presented in supplementary Table S4. Industries and urban WWTP discharge effluents rich in zinc directly into river. Large quantities of zinc-rich solid waste are also emitted into soils and the atmosphere by industry, urbanization and agriculture. The runoff and erosion from industrial, urban, and agricultural soils and atmospheric deposits releases large quantities of zinc into surface freshwater. As well as natural physical and chemical processes (see section 3), the processes used by humans to concentrate, extract or treat the zinc contained in natural materials will impact their $\delta^{66/64}$Zn value. In particular, high-temperature industrial processes, involving evaporation and condensation reactions with kinetic isotope effects, can induce significant isotopic fractionation between industrial and natural samples.

5.1 Mining and industrial activities

Zinc is widely dispersed in soils and the atmosphere because of past and current mining and industrial activity (supplementary Fig. S3). For example, according to IREP (Registre Français des Emissions Polluantes), 502 metric tons of zinc are emitted by industrial activity into soils and the atmosphere each year in France (2010-2017 average; http://www.irep.ecologie.gouv.fr/IREP/index.php). The main emitting activities are the production and smelting of metal, but also power plants (Gouzy and Brignon, 2014).

Industries also discharge metal-rich effluents directly into surface water. In France according to the IREP, 94 metric tons of zinc are emitted directly into surface water each year (2010-2017 average; http://www.irep.ecologie.gouv.fr/IREP/index.php). These come mainly from the metallurgy, surface treatment (e.g. electroplating, chemical deposit), and chemical industries.

5.1.1 Mining activities

Mining operations, in particular related to the extraction of sulfide minerals, cause enormous stocks of waste rock piles that contain notable residual Zn quantities. Samples collected in waste rock piles at sulfide mineral mines in the USA (Fe-Zn-Cu mine) and Peru (Cu-Zn-Mo mine) contained large quantities of zinc (up to 0.4% by mass)(Aranda et al., 2012; Skierszkan et al., 2016). The water percolating through these waste rock piles (i.e. effluent) can be also rich in zinc. Skierszkan et al. (2016) showed that experimental waste-rock weathering can produce effluents with high Zn content (up to 16 mg/L). The $\delta^{66/64}$Zn values for these samples are shown in Fig. S4. The Zn isotope compositions of various samples (solid waste and effluent) generally had values between +0.18 and +0.28‰ (n = 34, IQR, Fig. S3), which are consistent with those of sulfide mineralizations (+0.05 and +0.26‰, n = 294, IQR).

This similarity in $\delta^{66/64}$Zn values between mining residue and ores is because these residues have an isotope signature similar to the mineralizations that they accompany and the zinc in solution in effluents results from the dissolution of zinc-rich minerals, so this process only causes low enrichment of the isotope composition of the solution relative to the solid (Fig. 1).

5.1.2 Industrial activities

Metallurgical processes. The extraction of non-ferrous metals produces enormous quantities of waste called tailings. This solid waste can contain several % by mass of zinc (Bigalke et al., 2010; Juillot et al., 2011; Sivry et al., 2008). The particles emitted by smelter chimneys contain several hundreds of mg/kg of zinc (Mattielli et al., 2009). In general, for

high-temperature zinc pyrometallurgy processes in smelters, the zinc recovery yield is close to 100%, so the isotope fractionation between the ore and the resulting metal is low (Shiel et al., 2010; Sonke et al., 2008). John et al. (2007b) showed that the zinc in diverse metal parts (money, raw metals, etc.) has a range of isotope variations (between +0.09 and +0.31‰, n = 14) similar to that of ores (between +0.05 and +0.26‰, n = 294, IQR). Shiel et al. (2010) also showed by analyzing refined zinc alloy produced in Zn-Pb refining that the fractionation between the ore used (+0.17 ± 0.06‰) and the alloy produced (+0.22 ± 0.06‰) is low. Using these data for zinc metal, a signature for "common zinc" is defined between +0.15 and +0.22‰, and a median value of +0.19‰ (n = 15, IQR) (Fig. S3 and Fig. S4). Because of evaporation and condensation reactions that occur during the extraction process, waste from the operations (slags) have a considerably higher isotope signature (up to +1.5‰) (Bigalke et al., 2010; Couder et al., 2008; Juillot et al., 2011; Sivry et al., 2008; Yin et al., 2018), and particles emitted have a very low signature (up to -0.7‰) (Mattielli et al., 2009) compared to ores (between +0.05 and +0.26‰, n = 294, IQR) (Fig. S4). From analyzing various waste and products in metallurgic sites in France, a kinetic fractionation factor has been calculated for Rayleigh evaporation of zinc during refining ($\alpha_{solid\text{-}vapor}$) that is generally between 1.0001 and 1.0004 (Mattielli et al., 2009; Sivry et al., 2008). By following a Rayleigh model (Wiederhold, 2015), simulating the $\delta^{66/64}$Zn variations in separated and accumulated vapor and solid residue, it is possible to estimate the Zn isotope composition in waste produced during the smelting operations:

$$\delta_{slag} = \delta_{ore} + \varepsilon_{vapor-solid}\, lnf;\ \delta_{cumul\,vapor} = \delta_{ore} + \varepsilon_{vapor-solid}\, lnf - \frac{\varepsilon_{vapor-solid} lnf}{1-f} \quad (1)$$

Where $\varepsilon_{vapor\text{-}solid}$ is the isotope enrichment factor (‰) with $\varepsilon_{vapor\text{-}solid} \approx$ -1000 ln $\alpha_{solid\text{-}vapor}$ and *f* the fraction remaining.

For a starting composition of $\delta^{66/64}$Zn in ores between +0.05 and +0.26‰ (n=294, IQR), a $\alpha_{solid\text{-}vapor}$ fractionation factor between 1.0001 and 1.0004 and assuming a recovery of 98% for pure zinc production in smelting processes, the estimated $\delta^{66/64}$Zn values are between +0.44

559 and +1.82‰ for slags and -0.34 and +0.16‰ for particles (Fig. S4). These values are
560 consistent with slags and particles reported in previous studies (Bigalke et al., 2010; Couder
561 et al., 2008; Juillot et al., 2011; Mattielli et al., 2009; Sivry et al., 2008; Yin et al., 2018).
562 Water that percolates through slag tailings (between +0.51 and +1.40‰, n=4, Fig. S4) has a
563 similar isotope signature to slags (between +0.50 and +0.78‰, n=12, IQR, Fig. S3) (Shiel et
564 al., 2010; Sivry et al., 2008). These similar signatures for slag and effluents are related to the
565 fact that dissolution processes only cause low isotope fractionation of dissolved fraction
566 relative to the solid (Fig. 1). However, metallurgical slags are very heterogeneous materials,
567 composed of many mineral phases: mainly glassy phases but also crystalline phases like
568 spinels (franklinite ($ZnFe_2O_4$), gahnite ($ZnAl_2O_4$)), silicates (willemite (Zn_2SiO_4)) and zinc
569 metal (Yin et al., 2018). Theoretical equilibrium isotopic factors show that the dissolution of
570 these phases leads to a wide range of Zn fractionation between aqueous Zn and minerals
571 phases (Fig. S1). Moreover, weathering experiments on slags with different pH, atmospheres
572 and contact times showed that because of the slags' heterogeneity (various amorphous
573 glassy and crystalline phases), and because of multiple low-temperature inorganic chemical
574 reactions (precipitation of secondary phase, coprecipitation, adsorption) that take place while
575 they are altered, the $\delta^{66/64}Zn$ values between the slags and the leachate may vary
576 considerably from one experiment to another (up to 3‰) (Yin et al., 2018).

577 Since zinc is a chalcophile element, it is found as an impurity in other sulfide minerals like
578 galena (PbS) and chalcopyrite ($CuFeS_2$). For instance, in the Cubatão industrial region in
579 Brazil, which holds various metallurgical industries, the particles present in the atmosphere
580 have a very low signature ($\delta^{66/64}Zn$ between -0.59 and -0.06‰, n = 10, Souto-Oliveira et al.,
581 2019, 2018) compared to that of mineralizations (between +0.05 and +0.26‰, n = 294, IQR)
582 and similar to that of particles emitted by zinc smelters (between -0.38 and +0.05‰, n = 17,
583 IQR, Fig. S3). Zinc is also present in slags produced during lead production (up to 9% by
584 mass) (Gelly et al., 2019). In their study of a former lead smelter in the south of France, Gelly
585 et al. (2019) showed that Zn isotope compositions in slags have low values (between -0.04

and +0.18‰, n=8) compared to those of the slags analyzed in previous studies on zinc smelters (between +0.50 and +0.78‰, n=12, IQR) (Fig. S4). The same applies for the slags produced in a lead blast furnace in the north of France, whose Zn isotope composition (+0.13 ± 0.06‰, Yin et al., 2018) is similar to those in the tailings analyzed by Gelly et al., 2019. This depletion is likely not due to the starting material, i.e. galena that has a mean $\delta^{66/64}$Zn value (+0.23 ± 0.12‰, 2σ, n=8) close to that of other sulfide ores (+0.16 ± 0.48‰, 2σ, n=294) (Fig. 2). This is likely related to a different yield for this process, whose aim was not to recover the zinc.

Galvanization. Zinc is also used widely to protect metallic parts from corrosion. Zinc can be deposited on the part by submerging it in a liquid bath of molten zinc ("hot-dip" galvanization) or by electrolytic deposit (electroplating). John et al., (2007b) showed that galvanized objects have an isotope signature (between +0.12 and +0.58‰, n=3) similar to the levels in ores (between +0.05 and +0.26‰, n=294, IQR) and "common zinc" (between +0.15 and +0.22‰, n=15, IQR), whereas the parts with an electrolytic deposit have a strongly depleted signature (up to -0.60‰) (Fig. S4). This result was confirmed by laboratory experiments, which also showed depletion of the metal deposited that leads to enrichment of liquid bath with kinetic fractionation ($\alpha_{solution-metal}$) between 1.0010 and 1.0020 (Black et al., 2014; Kavner et al., 2008). This fractionation is likely due to that fact that not all the zinc present in the electrolytic bath is electrodeposited during this process (60% recovery) and that the light isotopes are preferably electrodeposited (Black et al., 2014; Kavner et al., 2008). By following a Rayleigh model (see equation 1), using a starting isotope composition close to that of ores (between +0.05 and + 0.26‰, n = 294, IQR), kinetic fractionation ($\alpha_{solution-solid}$) between 1.0010 and 1.0020 and a 60% recovery yield, the estimated values for $\delta^{66/64}$Zn in the electrodeposited metal are between -1.17 and -0.35‰, which is similar to the $\delta^{66/64}$Zn values obtained for commercial electrodeposited (screw and chain) zinc-coated articles (between -0.34 and -0.20‰, n = 3, John et al., 2007b) (Fig. S4).

Coal and waste combustion in power plants. The combustion of coal and waste in power plants releases high Zn contents into the atmosphere. Fly ash and flue gases sampled in coal-fired power plants and waste incineration plants contain large proportions of zinc (up to 3% by mass, Cloquet et al., 2006; Novak et al., 2016). While smelters operate between 600 °C and 700 °C, in coal-fired power plants, coal is combusted at higher temperatures (from 1200 to 1500 °C). At those temperatures, most of the zinc evaporates and condenses onto the fly ash particles, which are removed in electrostatic precipitators (ESPs) (Ochoa Gonzalez and Weiss, 2015). Although ESPs exhibit good retention for large particles, their efficiency is significantly lower for particles smaller than 0.8 µm remaining in flue gases and about 50% of the starting zinc is emitted through the stack (Ochoa Gonzalez and Weiss, 2015). The signatures in the fly gas are controlled by condensation processes with isotope fractionation kinetic factors ($\alpha_{solid-vapor}$) ranging between 1.0003 and 1.0007 (Ochoa Gonzalez and Weiss, 2015). From the analysis of fly ash and bottom ash samples coming from three power plants in Spain, Ochoa Gonzalez and Weiss (2015) predicted that the incineration of coal and pet coke with $\delta^{66/64}$Zn between +1.05 and +1.50‰ leads to zinc emission through the plant stack between +0.96 and +1.27‰. By following a Rayleigh model (see equation 1), for a starting composition of $\delta^{66/64}$Zn in coal between -0.10 and +1.35‰ (n=14, IQR), an $\alpha_{solid-vapor}$ factor between 1.0003 and 1.0007 and assuming a loss of 50% of zinc in the flue gas, $\delta^{66/64}$Zn values are estimated between -0.31 and +1.26‰ for zinc emission (Fig. S4). The Zn isotope signatures of flue gases from French urban waste incineration are between +0.07 and +0.19‰ (n = 3, Cloquet et al., 2006). These values match the estimated Zn isotope compositions for flue gases (between -0.06 and +0.13‰) obtained from incinerating material having an isotope signature similar to that of “common zinc” (between +0.15 and +0.22‰, n = 15, IQR) under the conditions set out previously ($\alpha_{solid-vapor}$ =1.0003 -1.0007, a loss of 50%) (Fig. S4).

In conclusion, the zinc emitted by coal-fired power plants and waste incineration plants has an isotope signature that is highly dependent on the combustible material. Given that the

coal has very variable $\delta^{66/64}$Zn values (-0.10 and +1.35‰, n = 14, IQR), Zn isotope compositions emitted when coal is combusted will also be very variable (estimated values between -0.31 and +1.26‰) with values that include the BSE (+0.28 ± 0.05‰, 2σ) and sulfide ore (between +0.05 and + 0.26‰, n=294, IQR) ranges. For waste incineration, if we consider that the starting materials have a signature similar to "common zinc" (between +0.15 and +0.22‰, n = 15, IQR), the variation in Zn isotope compositions in the particles emitted will be narrower (value estimated between -0.06 and +0.13‰) with lower values than ores (between +0.05 and +0.26‰, n = 294, IQR).

Other industries. As zinc metal is widespread in hardware, chemical components and organic materials, liquid effluents discharged into surface water by industries that do not work Zn metal as core processes (e.g. the chemical and agro-food industries), also contain high quantities of dissolved zinc (up to 500 µg/L, Table S1). Effluents coming from various industries (hospitals, chemicals, agro-food and surface treatment industries) are presented in supplementary Fig. S4 (this study). Industrial effluents have values for $\delta^{66/64}$Zn generally between +0.10 and +0.15‰ (n=7, IQR, Fig. S3), lower than the BSE value (+0.28 ± 0.05‰, 2σ) and close to that of "common zinc" (between +0.15 and +0.22‰, n = 15, IQR).

5.2 Emission from urban activities

Rivers can be strongly impacted by urban pressure (urban WWTP, zinc roofing, road traffic). Urban WWTP discharge metal-rich effluents directly into surface water. For example, in France, according to the IREP, 69 metric tons of zinc are emitted each year directly into surface water by urban WWTP (2010-2017 average; http://www.irep.ecologie.gouv.fr/IREP/index.php). Galvanized zinc is widely used to cover roofs and weathering caused by rainwater carries large quantities of zinc into rivers. Gouzy and Brignon (2014) estimated that 6 metric tons of zinc are discharged each year into surface water in France due to zinc roofing. Road traffic is also a substantial zinc emitter, through engines (gasoline), vehicle wear and tear (brakes, tires) and roadway equipment (safety barriers). As an example, CITEPA (Centre Interprofessionnel Technique d'Etudes de

la Pollution Atmosphérique) estimates that about 300 metric tons of zinc is emitted into the atmosphere each year in France due to road traffic (Data: https://www.citepa.org/fr/air-et-climat/polluants/metaux-lourds/zinc).

5.2.1 Urban wastewater treatment plants (WWTP)

Urban WWTP effluents can contain high quantities of dissolved zinc (up to 200 µg/L, Table S1). The Zn concentrations and $\delta^{66/64}$Zn values for raw wastewater and effluents coming from medium WWTP (10,000 to 100,000 Population Equivalent (PE)) and large WWTP (> 100,000 PE) are presented in Fig. S5 (Chen et al., 2008, this study). Treated wastewater coming from various WWTP have values for $\delta^{66/64}$Zn generally between +0.06 and +0.08‰ (n=5, IQR, Fig. S3), close to industrial effluents (+0.10 and +0.15‰, n=7, IQR) and lower than the $\delta^{66/64}$Zn values for raw wastewater (+0.28 ± 0.02‰, n = 1) and the BSE value (+0.28 ± 0.05‰, 2σ). Previous study showed that dissolved Zn in WWTP effluent is mainly organically complexed to organic ligands (Chaminda et al., 2013). However, the $\delta^{66/64}$Zn for WWTP effluents depleted in heavy isotopes compared to wastewater is not consistent with a change in speciation, which tends to enrich in heavy isotopes organic complexed Zn compared to free Zn^{2+} (see section 3).

In WWTP, wastewaters undergoes various treatment stages (primary settling, secondary activated sludge and tertiary flocculation by $FeCl_3$) to decrease particulate metal concentrations (Buzier et al., 2006). However, several studies have shown that the dissolved metal content increases along with the wastewater treatment steps in WWTP (Buzier et al., 2006; Gourlay-Francé et al., 2011). According to Gourlay-Francé et al. (2011), various assumptions may explain this increasing dissolved Zn concentration during the wastewater treatment steps: (1) metal desorption from particles and organic matter, (2) dissolution of iron salts added during the dephosphorization treatment, e.g. $FeCl_3$ containing high trace metal concentrations. Previous studies have reported that the heavier isotopes are preferentially adsorbed onto organic matter, clays and oxides (Fig. 1), so zinc desorption from particles

693 and organic matter should enrich the solution in heavy Zn isotopes. Therefore, treated
694 wastewater's depletion in heavy isotopes compared to untreated wastewater cannot be due
695 to a simple desorption process. Zinc-rich chemical components dissolving during wastewater
696 treatment, depleted in heavy isotopes compared to untreated wastewater, may explain this
697 result. For example, the $\delta^{66/64}$Zn signature of ferric chloride may be depleted in heavy
698 isotopes due to isotope fractionation during its industrial production process (see section
699 5.1.2), or to the initial Fe ore used in this process, which may be, like Zn ores, lower
700 (+0.16‰, n = 294) than the BSE value (0.28 ± 0.05‰, 2σ). Determine the $\delta^{66/64}$Zn signature
701 of ferric chloride would be necessary to verify that it is the addition of zinc-rich chemical
702 components with low $\delta^{66/64}$Zn value, which explains the lower $\delta^{66/64}$Zn values for the effluents
703 produced by WWTP (+0.06 and +0.08‰, n=5, IQR) relative to the BSE value (0.28 ± 0.05‰,
704 2σ).
705
706 ### 5.2.2 Zinc roofing
707 In their study of the Seine watershed, Chen et al. (2008) analyzed roof runoff samples
708 collected in the Paris conurbation, known for its zinc roofs. They analyzed also leached
709 samples of zinc roof coverings. These samples contain high Zn contents (up to 2 mg/L for
710 roof runoffs and 92 mg/L for leached sample) and their Zn isotope compositions ($\delta^{66/64}$Zn) are
711 generally low (between -0.10 and -0.02‰, n = 5, IRQ, Chen et al., 2008, Fig.S3) compared to
712 that of "common zinc" (between +0.15 and +0.22‰, n = 15, IQR).
713 This difference of $\delta^{66/64}$Zn values between "common zinc" and roof runoff samples is not
714 consistent with fractionations due to metallic zinc dissolution, which tends to enrich the
715 dissolved Zn^{2+} relative to metal Zn (Fig. S1). These differences can be due to the starting
716 material (electrodeposited zinc?), or to a contribution from particles of industrial origin (see
717 section 5.1.2).
718

5.2.3 Road traffic

Zinc emitted by road traffic can be due to non-exhaust emissions (Brake pad liners, tires, roadway equipment) and exhaust emissions (gasoline).

Non-exhaust emissions. Brake pad liners contain a large quantity of zinc (up 2% by mass) mainly in the form of metal (brass), but also zinc oxide and sulfide (ZnO, ZnS, etc.) (Blau, 2001; Hjortenkrans et al., 2007; Legret and Pagotto, 1999). Zn isotope compositions for non-exhaust emissions are shown in Fig. S5. The mean $\delta^{66/64}$Zn value for brake pads sold in France and the UK is 0.19 ± 0.08‰ (2σ, n=3, Dong et al., 2017; this study). This value is similar to "common zinc" (between +0.15 and +0.22‰, n=15, IQR), which matches the fact that zinc in the brake pads is mainly present in metal form. During tire production, zinc is added to the rubber in oxide form (ZnO) and also low quantities in the form of organo-zinc compounds to facilitate vulcanization. Tires also generally contain about 1% by mass of zinc (Councell et al., 2004; Legret and Pagotto, 1999). Zn isotope compositions in tires from the USA, Brazil and the UK generally vary between +0.08 and +0.21‰ with a median value of 0.13‰ (n = 15, IQR, Dong et al., 2017; Souto-Oliveira et al., 2018; Thapalia et al., 2010, Fig. S3). This slightly lower value than "common zinc" (between +0.15 and +0.22‰, n = 15, IQR) is probably related to fractionation during production of tires or raw materials used during vulcanization. Safety barriers at roadsides are coated with zinc by hot galvanization (standard ISO 1461). No analysis of safety barriers is available in the literature, however since they are hot-galvanized, their Zn isotope compositions ought to be similar to that of "common zinc" (between +0.15 and +0.22‰, n = 15, IQR).

Exhaust emissions. Compared with non-exhaust emissions, gasolines contain zinc, added as additive, in a lower quantity (up to 150 µg/L of zinc, Barbusse and Plassat, 2005; Nomngongo and Ngila, 2014). Zn isotope compositions in gasolines between -0.50 and -0.23‰ (n=2, Gioia et al., 2008) are very low compared with values in tires and brakes (Fig. S5). It is important to note that when fuel combusts in evaporation/condensation reactions it

745 will also tend to reduce this heavy isotope signature compared to its initial composition (See
746 section 5.1.2).

747

748 ## 5.3. Zinc emissions from agricultural activities

749 Agricultural operations like animal and arable farming concentrate high quantities of metals,
750 particularly of zinc, which accumulate in the soil's surface layer. Sprayed inorganic and
751 organic fertilizers, and crop protection treatments, especially for vines, are particular zinc
752 sources (Gouzy and Brignon, 2014). From a study of contamination sources in agricultural
753 land and how those are used, Belon et al. (2007) have estimated that on average 0.514 kg of
754 zinc are applied each year per hectare of Utilized Agricultural Area. For example, in France,
755 14,906 metric tons of zinc is sprayed each year on 29 million hectares of agricultural land.
756 The portion of substance emitted on agricultural land that reaches surface water by runoff
757 was estimated between 0.1 and 1% (mean of 0.4%) by Braun et al. (2000). From this
758 estimate, it is possible to calculate that each year about 60 metric tons of zinc is added to
759 surface water in metropolitan France because of agricultural activity.

760 ### Fertilizers

761 Sewage sludge from water treatment plants used as fertilizers generally contains more than
762 500 mg/kg of zinc (Eriksson, 2001; Meeddat, 2009). Organic fertilizers also include animal
763 waste from manure and slurry. Effluents from pig farming contain several hundreds of mg/kg
764 of zinc (Eriksson, 2001; Levasseur, 2005; Nicholson et al., 1999). These high contents are
765 due to nutritional supplements with particularly high Zn contents that are given to animals to
766 promote growth, but also supplied from weathering galvanized metal parts present in
767 industrial farming (grating, tubes, etc.) (Levasseur, 2005; Levasseur and Texier, 2001; Smith
768 et al., 1962). Manure generally has lower metal concentrations than slurries, because it is
769 diluted by hay provided that contains little metals. Bovine feces contains less zinc (around
770 100 mg/kg) than pig feces, but cattle producing almost 10 times as much excrement as pigs

771 (Brassard et al., 2012; Eriksson, 2001; Nicholson et al., 1999). With Zn contents of the order
772 of a few tens of mg/kg, inorganic fertilizers have lower Zn concentrations than organic
773 fertilizers and their concentration varies widely, even in products coming from a single
774 manufacturer (Eriksson, 2001). The isotope compositions for various fertilizers are shown in
775 supplementary Fig. S5. The range of variation for "common zinc" (between +0.15 and
776 +0.22‰, n = 15, IQR) is also shown because of the many galvanized hardware present in
777 farms. Since we do not have data on nutritional supplements given to pigs, we used the
778 values for $\delta^{66/64}$Zn supplements intended for humans. These health products have quite
779 variable Zn isotope compositions with $\delta^{66/64}$Zn values between +0.10 and +0.20‰ (n = 5,
780 IQR, John et al., 2007b, Fig. S3). A study conducted by Balter et al. (2010) on sheep showed
781 that Zn isotope signatures in urine and feces of an animal are similar to that of their food. The
782 only manure analyzed (this study) has an isotope signature (+0.31 ± 0.03‰, n = 1) similar to
783 that of BSE (+0.28 ± 0.05‰, 2σ). It is therefore likely from an animal that was fed with feed
784 having a geogenic signature, without any nutritional supplement, which would have a lighter
785 isotope composition (John et al., 2007b) (Fig. S5). The sewage sludge analyzed by Chen et
786 al. (2008) also has a Zn isotope signature (+0.31 ± 0.02‰, n = 1) similar to that of BSE
787 (+0.28 ± 0.05‰, 2σ). Pig slurries have $\delta^{66/64}$Zn values between +0.07 and +0.24‰ (n = 3)
788 (Fekiacova et al., 2015; this study), which likely reflect both the Zn isotope composition of the
789 animal feed with varying supplements with variable $\delta^{66/64}$Zn values (between +0.10 and
790 +0.20‰, n = 5, IQR), but also reflect runoff from metal parts on the farm ("common zinc"
791 between +0.15 and +0.22‰, n = 15, IQR).

792 $\delta^{66/64}$Zn values for inorganic fertilizers vary widely (between -0.06 and +0.42‰, n = 4, Chen
793 et al., 2008; Szynkiewicz and Borrok, 2016) (Fig. S5).

794 **Crop protection treatments**

795 Vineyards are treated by either copper-based fungicides, such as Bordeaux mixture
796 [($CuSO_4 \cdot 5H_2O$ + $Ca(OH)_2$)], or other fungicides containing zinc, such as Mancozeb, a

dithiocarbamate ($C_8H_{12}MnN_4S_8Zn$) (da Rosa Couto et al., 2015). Until now, no Zn isotope analysis has been carried out on these products. The Bordeaux mixture has been widely used in European vineyards since the end of the 19th century. Copper sulfate used in preparing the Bordeaux mixture may contain significant amounts of zinc (Duplay et al., 2014). Copper sulfate is produced industrially by treating copper metal with hot concentrated sulfuric acid or its oxides with dilute sulfuric acid. Chalcopyrite has $\delta^{66/64}$Zn values generally between -0.09 and +0.19‰ (n=11, IQR, Fig. S2), however given that fractionation can occur during the extraction of copper or the production of copper oxides and sulfates, we cannot use these values as a representative of the Bordeaux mixture.

6 Application of zinc isotopes to trace sources and fate of zinc in rivers

Fig. 4 summarizes Zn isotope compositions for various anthropogenic contributions compared to the BSE signature (+0.28 ± 0.05‰, 2σ) and to non-impacted rivers (GBSW, between +0.24 and 0.41‰, n = 127, IQR). In Fig. 4, contributions are represented by a box-plot when they are composed of more than four pieces of data. The distribution of data for the various anthropogenic contributions is in Fig. S3. The capacity of Zn isotopes to track anthropogenic contributions (mines, metallurgy, urbanization, agriculture) in surface water was applied and investigated by various studies described below.

6.1 Rivers impacted by mining activity

Rivers and groundwater in mining zones can have very high dissolved Zn concentrations (up to 70 mg/L) and $\delta^{66/64}$Zn values generally between +0.01 and +0.29‰ (n = 99, IQR, Aranda et al., 2012; Balistrieri et al., 2008; Borrok et al., 2009; Szynkiewicz and Borrok, 2016; Wanty et al., 2013; this study) (Fig. 5). This range of $\delta^{66/64}$Zn values is very close to that of sulfide mineralizations (between +0.05 and +0.26‰, n = 294, IQR) and solid waste and effluents present in mining areas (between +0.18 and +0.28‰, n=34, IQR). These similar isotope

signatures are due to the fact that zinc in solution in rivers and groundwater results from the dissolution of zinc-rich minerals contained in ores and tailings, so this process only slightly enriches the solution (Fig. 1). However, $\delta^{66/64}Zn$ values have lower heavy isotope levels for samples from Sardinia (-0.10 ± 0.24‰, 2σ, n = 10) compared with other water courses impacted by mining activity (0.16 ± 0.42‰, 2σ, n = 89) (Fig. 5). Wanty et al. (2013) state that these signatures are due to the biologically-mediated production of hydrozincite ($Zn_5(CO_3)_2(OH)_6$), which concentrates heavy isotopes. These results are consistent with laboratory experiments and theoretical data, which showed that hydrozincite precipitation tends to reduce the $\delta^{66/64}Zn_{dissolved}$ value relative to precipitate (see section 3). In conclusion, Zn isotope signatures for rivers impacted by mining activity are close to those of natural water. This precludes the use of Zn isotopes to track mining pollution in rivers. However, Zn isotope compositions are a valuable tool for highlighting secondary processes (dissolution, precipitation, etc.) between particulate and dissolved phases (Aranda et al., 2012; Skierszkan et al., 2016; Veeramani et al., 2015; Wanty et al., 2013), which control the attenuation and release of zinc in surface water.

6.2 Rivers impacted by industrial activity

In their studies in the Sepetiba Bay (Brazil), Araújo et al. (2018, 2017a, 2017b) used Zn isotope compositions for core samples of stream sediments and SPM to reconstitute a timeline for changes in zinc contamination related to industrial metallurgy. From studying core samples of stream sediment, Sivry et al. (2008) and Petit et al. (2015) have also shown how zinc ore-smelter activity affects the river Lot's watershed (France). In Fig. 6, the data from these studies are mixtures between a natural GBSW contribution and an anthropogenic contribution seen in the slags that is related to metallurgic activity. To date no dedicated study has been published on how industrial metallurgy activity impacts the Zn isotope signature in solution in surface water. However, a recent laboratory study on lixiviation of slags showed great diversity in Zn isotope signatures in the lixiviates (See section 5.1.2, Yin

et al., 2018). The use of Zn isotope compositions to trace the impact of metallurgic activity in surface water must therefore be considered with precaution.

The contribution of atmospheric particles from metallurgical industries can be evaluated in urban aerosols because of their very low signature (between -0.38 and +0.05‰, n = 17, IQR) compared to the GBSW (between +0.24 and +0.41‰, n=127, IQR) (Dong et al., 2017; Souto-Oliveira et al., 2019, 2018). However, it is more difficult to establish the contribution of these atmospheric particles in surface water because of the physical and chemical processes (adsorption, precipitation, etc.) that take place in water (see section 3) modifying their Zn isotope signature.

Regarding the effluents discharged by different types of industries, their depleted signatures (between +0.10 and +0.15‰, n=7, IQR) compared to the GBSW (between +0.24 and 0.41‰, n = 127, IQR) ought to allow them to be traced in surface water (see section 5.1.2 concerning industrial effluents).

6.3 Rivers impacted by urbanization

Urbanization impacts surface water for several known reasons. One is point-source discharges in the form of effluents from large WWTP; another is release by runoff and/or erosion of zinc contained in emissions related to road traffic and runoff on zinc-coated roofs. In their study on the Seine basin, Chen et al. (2008) showed how urbanization has impacted Zn isotope compositions in the river's dissolved phase (Fig. 7). For zinc in solution present in the Loire, even though the contents are low (+1.3 ± 0.8 µg/L, 2σ, n=10, this study) (Table S2), we see slight decreases in $\delta^{66/64}$Zn from upstream to downstream (Fig. 7). The same applies for sediments and SPM taken from urban rivers and lakes (Araújo et al., 2019; Chen et al., 2009b; Petit et al., 2015, 2008; Thapalia et al., 2015, 2010; this study), where increased Zn content is accompanied by a lower $\delta^{66/64}$Zn value (Fig. 7). Fig. 7 shows that though the contribution of roof runoff may be excluded in these samples, they correspond to

mixtures of a natural GBSW contribution and an anthropogenic contribution due to WWTP effluents and/or non-exhaust road traffic emissions.

6.4 Rivers impacted by agricultural activity

As previously stated, little data exists on Zn isotope compositions in agricultural contamination sources (fertilizer and crop protection treatment). For French watersheds that mainly hold arable and animal farming land we see that sediments and SPM may contain high Zn contents (up to 417 mg/kg) (Table S3), but their isotope composition is similar (0.27 ± 0.06‰, 2σ, n = 6, this study) to the GBSW (between +0.24 and 0.41‰, n=127, IQR) (Fig. 8). This result matches Zn isotope compositions in organic fertilizers, which show similar $\delta^{66/64}$Zn values (between +0.21 and +0.31‰, n = 5, IQR) to GBSW (between +0.24 and +0.41‰, n = 127, IQR) (Fig. S5).

6.5 Towards a multi-isotopic approach

Many studies have successful used a multi-isotope approach, i.e. Zn isotopes combined with other metals (Pb, Cu, etc.) to track the origin of pollution in soils and in atmospheric particles (e.g. Gelly et al., 2019; Souto-Oliveira et al., 2018). In rivers and lakes, due to the same chemical separation protocol, analyses of Zn isotopes are associated with Cu isotopes in several studies (Araújo et al., 2019; Balistrieri et al., 2008; Guinoiseau et al., 2018, 2017; Petit et al., 2008; Thapalia et al., 2010; Vance et al., 2016). Combining measurements of stable Cu and Zn isotopes may be helpful for identifying the exchange processes between the particulate and dissolved fractions in river. Aebischer et al. (2015) used a multi-isotopic approach (Zn, Fe, and Pb) in lake sediments impacted by multiple pollution sources (mining, urban, industrial, gasoline). This study highlighted the potential of a multi-isotope approach to identify metal sources and pathways. However, even though it is a powerful tool, especially in soils and atmospheric particles, the multi-isotopic approach should be used with caution in

902 an aquatic environment. The elements used must have a common source and have close
903 chemical properties to be transported in similar ways in aqueous media. Another important
904 factor to consider is post-depositional processes, which can induce substantial isotopic
905 variability according to the element and can hide the initial source signatures.

906
907
908 ## 7 Summary and future directions

909 Though zinc is essential for life, in excess it may be toxic to organisms. In addition to natural
910 zinc sources, many human activities mobilize and spread large quantities of zinc in the
911 environment (i.e. industry, agriculture, road traffic and treated domestic effluents).
912 Discriminating the various natural and anthropogenic zinc sources in the environment, as
913 well as understanding zinc's fate at a catchment scale in both dissolved and solid phases, is
914 a key challenge in order to take the appropriate measures to prevent degradation of the
915 aquatic environment. Isotope approaches, especially for lead, have proven their efficiency in
916 tracing sources in the environment for decades. Compared to these "traditional" isotopes, the
917 worth of tracing with Zn isotopes, more recently developed (2000s), has still to be proven.
918 This review compiles the major findings of previous studies in order to evaluate the ability of
919 Zn isotope compositions to trace metal sources at a catchment scale.

920 First of all, we presented the isotope fractionations due to the interactions between minerals
921 or live organisms and aqueous solutions that control how zinc is distributed between the
922 dissolved and particulate phases in surface water and can modify the $\delta^{66/64}$Zn initial
923 signatures of anthropogenic zinc sources. Though dissolution processes seem to slightly
924 fractionate Zn isotope signatures (-0.2 - 0.0‰), the adsorption of zinc on mineral particulate
925 phases as well as its complexation onto organic compounds decreases $\delta^{66/64}$Zn in the
926 remaining solution (~ +0.30‰). Precipitation could increase or decrease $\delta^{66/64}$Zn in the
927 remaining solution depending on the nature of the newly formed zinc-bearing minerals.

928 Uptake by plants and microorganisms generally increases the $\delta^{66/64}Zn_{dissolved}$ when the
929 concentration of free ions in the nutrient solution is high (>~10 µg/L).

930 Secondly, we summarized available data for the main natural sources of zinc, to define (1)
931 the bulk silicate earth signature (BSE, $\delta^{66/64}Zn$ = +0.28 ± 0.05‰ (2σ)); (2) the zinc-sulfide ore
932 deposit signature $\delta^{66/64}Zn$ = +0.05 to +0.26‰, with a mean (or median) value of +0.16‰; (3)
933 coal signatures that are highly variable $\delta^{66/64}Zn$ = -0.10 to +1.35‰ depending on the
934 diagenetic processes involved. Rivers draining natural environments generally have low
935 dissolved Zn concentrations (<2 µg/L) and about 200 mg/kg in the particulate phases
936 (sediments and SPM). Zn isotope compositions in natural water, SPM and sediments vary
937 slightly and are used to define the "geological background for surface water" (GBSW, $\delta^{66/64}Zn$
938 = +0.24 to +0.41‰ with a median value of +0.30‰) that is close to the BSE value.

939 Thirdly, the main zinc anthropogenic inputs, with their respective Zn isotope signatures as
940 well as the main processes leading to these specific isotope characteristics, can be
941 summarized as follows: (1) Solid wastes and effluents produced during mining activities have
942 $\delta^{66/64}Zn$ values between +0.18 and +0.28‰, close to GBSW and zinc sulfide ore values; (2)
943 Slags and water leaching the slag tailings have $\delta^{66/64}Zn$ values between +0.51 and +1.20‰,
944 higher than the GBSW values due to condensation and evaporation processes during
945 smelting processes. Conversely, particles emitted by smelters into the atmosphere are
946 strongly depleted in heavy isotopes, $\delta^{66/64}Zn$ = -0.38 to +0.05‰ compared to GBSW values;
947 (3) Industrial effluents (chemical industry, agro-food industry) have $\delta^{66/64}Zn$ between +0.10
948 and +0.15‰, lower than the GBSW values; (4) Electroplated zinc has an isotope signature of
949 $\delta^{66/64}Zn$ = -0.56 to -0.20‰, depleted in heavy isotopes relative to GBSW values because of
950 isotope fractionation during the process, while zinc plated by hot-dip galvanization should
951 have $\delta^{66/64}Zn$ values close to "common zinc" (+0.15 to +0.22‰), slightly depleted in heavy
952 isotopes compared to GBSW values; (5) Particles released into the atmosphere from
953 combustion in power plants should present wide $\delta^{66/64}Zn$ variation because of the isotope
954 variability of the burned material. For instance, the $\delta^{66/64}Zn$ of coal varies between -0.10 and

+1.35‰, and covers the range of GBSW values; (6) Treated wastewater effluents have $\delta^{66/64}$Zn between +0.06 and +0.08‰, lower than the GBSW values, possibly due to zinc-rich chemicals added during water treatment processes; (7) The $\delta^{66/64}$Zn for zinc roof runoff is lower (-0.10 to -0.02‰) compared to GBSW values; (8) Non-exhaust emissions resulting from road traffic have $\delta^{66/64}$Zn = +0.11 to +0.21‰, slightly depleted in heavy isotopes compared with GBSW values. Note that non-exhaust emissions and zinc-plated by hot-dip galvanization have close $\delta^{66/64}$Zn values because they are both derived from "common Zn". The little data available for gasoline show that $\delta^{66/64}$Zn are strongly depleted in heavy isotopes (between -0.50 and -0.23‰) compared to GBSW values; finally; (9) Organic fertilizers have $\delta^{66/64}$Zn values = +0.21 to +0.31‰ close to the GBSW values. Mineral fertilizers have wide variations (-0.06 to +0.42‰) that cover the range of GBSW values. Note that no data are available for crop protection treatments, which can have high Zn contents.

Finally, among the environmental studies based on Zn isotopes that track zinc sources in rivers:

(1) Rivers impacted by acid-mine drainage present, in addition to potentially high Zn concentrations, similar $\delta^{66/64}$Zn levels to sulfide mineralization because dissolution causes very little fractionation. However, secondary processes (e.g. precipitation and adsorption) can produce Zn isotope shifts.

(2) The impact of the metallurgical industry on river basins has been studied through solid materials (sedimentary cores, stream sediments and SPM) demonstrating that $\delta^{66/64}$Zn in these particulate phases results from mixing between the natural background and an anthropogenic end-member represented by slags. These studies showed that Zn isotope composition is a powerful tool for tracking the anthropogenic source of slags in particulate phases of rivers. No studies report data on the dissolved phase in rivers impacted by metallurgical activities; however, since the weathering of slags leads to a wide range of Zn isotope compositions, it seems that tracking their contribution in surface water would be impractical.

(3) The impact of urbanization includes several types of zinc sources (WWTP effluents, road-traffic emissions, and zinc-covered roof runoff). WWTP effluents and non-exhaust traffic emissions with their close $\delta^{66/64}$Zn signatures will be difficult to discriminate. The Zn isotope compositions for dissolved loads, sediments and SPM sampled in urban rivers and lakes are a mix between the natural background and an anthropogenic end-member represented by WWTP effluents, and/or non-exhaust road traffic emissions. Though not allowing a clear distinction between all types of urban zinc sources, $\delta^{66/64}$Zn signatures are an efficient tool for tracking a global urban contribution in rivers.

(4) The impact of agriculture is poorly documented to date. Though the scarce data available do not reveal significant isotope shifts compared to the GBSW, this needs to be further investigated as agriculture is a major source of diffuse zinc at a catchment scale.

On this basis, we highlight research needs and propose future work to make Zn isotopes a relevant tracer of zinc and associated trace metals sources and fate at a catchment scale:

(1) As has been done for lead isotopes, the Zn isotope characterization of anthropogenic sources needs to be further investigated. In particular, it will be necessary to increase the number of samples analyzed to create an exhaustive reference database. Zn emissions from agricultural activities, which are a major source of zinc at a catchment scale, have to be widely studied.

(2) Zn isotope fractionations linked to processes (biologically mediated or not) that control the distribution of metals between the dissolved and particulate phases in surface water need to be better understood. A multi-technique approach coupling Zn isotope signatures in natural and experimental samples with theoretical studies using *ab initio* calculations to predict isotope fractionation and X-ray absorption spectroscopy to establish zinc speciation will be necessary for understanding the dominant processes that play a role in zinc mobility.

(3) Anthropogenic metal releases into the environment often combine zinc with other metals (e.g. Cu in WWTP effluents and Pb in gasoline). In rivers impacted by multiple sources

of pollution, it is necessary to combine Zn isotopes with other metal isotopes to clearly evaluate the impact of various anthropogenic contributions. Moreover, coupling zinc and a combination of carefully selected metal isotopes would take us further in understanding the fate of metals in the different compartments of a river basin by constraining various physical and chemical processes governing the metal distributions between particulate and dissolved phases.

(4) Using new sampling techniques should be considered, for example passive DGT samplers (Diffusive gradients in thin films) to determine Zn isotope composition in surface water. DGT can pre-concentrate metals in situ and provide an isotope composition of water integrated over time. Moreover, DGT-measurable metal fractions are also considered as a proxy for the dissolved bioavailable metal fraction, which is a key factor when considering how metals impact the environment.

Acknowledgments

We are grateful to E. Decouchon, C. Innocent, D. Widory, J. Gattacceca and R. Millot for their help during sample collection and to S. Perret and R. Dupuy for sample preparation. Thanks are also due to N. Baran, M. Barnier and X. Bourrain for helpful discussions. This work was financially supported by BRGM, AQUAREF (BRGM, IFREMER, INERIS, IRSTEA, LNE) and the Agence de l'eau Loire-Bretagne. Karen M. Tkaczyk edited the final English version of the paper. R. Wanty, E. Skierszkan and anonymous reviewers are thanked for their constructive comments and highlights, which greatly helped to improve the manuscript.

References

Abanades, S., Flamant, G., Gagnepain, B., Gauthier, D., 2002. Fate of heavy metals during municipal solid waste incineration. Waste Manag. Res. 20, 55–68.

Aebischer, S., Cloquet, C., Carignan, J., Maurice, C., Pienitz, R., 2015. Disruption of the geochemical metal cycle during mining: Multiple isotope studies of lake sediments from Schefferville, subarctic Québec. Chem. Geol. 412, 167–178. https://doi.org/10.1016/j.chemgeo.2015.07.028

AELB, 2013. État des lieux du bassin Loire-Bretagne établi en application de la directive cadre sur l'eau.

Albarède, F., 2004. The stable isotope geochemistry of copper and zinc. Rev. Mineral. Geochemistry 55, 409–427. https://doi.org/10.2138/gsrmg.55.1.409

Aranda, S., Borrok, D.M., Wanty, R.B., Balistrieri, L.S., 2012. Zinc isotope investigation of surface and pore waters in a mountain watershed impacted by acid rock drainage. Sci. Total Environ. 420, 202–213. https://doi.org/10.1016/j.scitotenv.2012.01.015

Araújo, D.F., Boaventura, G.R., Machado, W., Viers, J., Weiss, D., Patchineelam, S.R., Ruiz, I., Rodrigues, A.P.C., Babinski, M., Dantas, E., 2017a. Tracing of anthropogenic zinc sources in coastal environments using stable isotope composition. Chem. Geol. 449, 226–235. https://doi.org/10.1016/j.chemgeo.2016.12.004

Araújo, D.F., Machado, W., Weiss, D., Mulholland, D.S., Boaventura, G.R., Viers, J., Garnier, J., Dantas, E.L., Babinski, M., 2017b. A critical examination of the possible application of zinc stable isotope ratios in bivalve mollusks and suspended particulate matter to trace zinc pollution in a tropical estuary. Environ. Pollut. 226, 41–47. https://doi.org/10.1016/j.envpol.2017.04.011

Araújo, D.F., Machado, W., Weiss, D., Mulholland, D.S., Garnier, J., Souto-Oliveira, C.E., Babinski, M., 2018. Zinc isotopes as tracers of anthropogenic sources and biogeochemical processes in contaminated mangroves. Appl. Geochemistry 95, 25–32. https://doi.org/10.1016/j.apgeochem.2018.05.008

Araújo, D.F., Ponzevera, E., Briant, N., Knoery, J., Sireau, T., Mojtahid, M., Metzger, E., Brach-Papa, C., 2019. Assessment of the metal contamination evolution in the Loire estuary using Cu and Zn stable isotopes and geochemical data in sediments. Mar. Pollut. Bull. 143, 12–23. https://doi.org/10.1016/j.marpolbul.2019.04.034

Archer, C., Vance, D., 2004. Mass discrimination correction in multiple-collector plasma source mass spectrometry: an example using Cu and Zn isotopes. J. Anal. At. Spectrom. 19, 656. https://doi.org/10.1039/b315853e

Archer, C., Vance, D., Butler, I., 2004. Abiotic Zn isotope fractionations associated with ZnS precipitation, in: Geochimica et Cosmochimica Acta Volume 68, Issue 11, Supplement. p. 325.

Arle, J., Mohaupt, V., Kirst, I., 2016. Monitoring of Surface Waters in Germany under the Water Framework Directive—A Review of Approaches, Methods and Results. Water 8, 217. https://doi.org/10.3390/w8060217

Arnold, T., Kirk, G.J.D., Wissuwa, M., Frei, M., Zhao, F.J., Mason, T.F.D., Weiss, D.J., 2010b. Evidence for the mechanisms of zinc uptake by rice using isotope fractionation. Plant, Cell Environ. 33, 370–381. https://doi.org/10.1111/j.1365-3040.2009.02085.x

Arnold, T., Markovic, T., Kirk, G.J.D., Schönbächler, M., Rehkämper, M., Zhao, F.J., Weiss,

1076 D.J., 2015. Iron and zinc isotope fractionation during uptake and translocation in rice
1077 (Oryza sativa) grown in oxic and anoxic soils. Comptes Rendus - Geosci. 347, 397–404.
1078 https://doi.org/10.1016/j.crte.2015.05.005

1079 Arnold, T., Schönbächler, M., Rehkämper, M., Dong, S., Zhao, F.J., Kirk, G.J.D., Coles, B.J.,
1080 Weiss, D.J., 2010a. Measurement of zinc stable isotope ratios in biogeochemical
1081 matrices by double-spike MC-ICPMS and determination of the isotope ratio pool
1082 available for plants from soil. Anal. Bioanal. Chem. 398, 3115–3125.
1083 https://doi.org/10.1007/s00216-010-4231-5

1084 Aucour, A.M., Bedell, J.P., Queyron, M., Magnin, V., Testemale, D., Sarret, G., 2015.
1085 Dynamics of Zn in an urban wetland soil-plant system: Coupling isotopic and EXAFS
1086 approaches. Geochim. Cosmochim. Acta 160, 55–69.
1087 https://doi.org/10.1016/j.gca.2015.03.040

1088 Aucour, A.M., Pichat, S., MacNair, M.R., Oger, P., 2011. Fractionation of stable zinc isotopes
1089 in the zinc hyperaccumulator arabidopsis halleri and nonaccumulator arabidopsis
1090 petraea. Environ. Sci. Technol. 45, 9212–9217. https://doi.org/10.1021/es200874x

1091 Balistrieri, L.S., Borrok, D.M., Wanty, R.B., Ridley, W.I., 2008. Fractionation of Cu and Zn
1092 isotopes during adsorption onto amorphous Fe(III) oxyhydroxide: Experimental mixing of
1093 acid rock drainage and ambient river water. Geochim. Cosmochim. Acta 72, 311–328.
1094 https://doi.org/10.1016/j.gca.2007.11.013

1095 Balter, V., Zazzo, A., Moloney, A.P., Moynier, F., Schmidt, O., Monahan, F.J., Albarède, F.,
1096 2010. Bodily variability of zinc natural isotope abundances in sheep. Rapid Commun.
1097 Mass Spectrom. 24, 3567–3577. https://doi.org/10.1002/rcm

1098 Ban, Y., Aida, M., Nomura, M., Fuji, Y., 2002. Zinc Isotope Separation by Ligand Exchange
1099 Chromatography Using Cation Exchange Resin. J. Ion Exch. 13, 46–52.
1100 https://doi.org/10.5182/jaie.13.46

1101 Barbusse, S., Plassat, G., 2005. Les particules de combustion automobile et leurs dispositifs
1102 d'élimination. Rapport ADEME.

1103 Belon, E., Boisson, M., Jardin, A.-S., Gaultier, G., Laura, D., Cabal, A., Ballester, R., 2007.
1104 Bilan des flux de contaminants entrant sur les sols agricoles de France
1105 métropolitaine.Rapport ADEME par SOGREAH.

1106 Bermin, J., Vance, D., Archer, C., Statham, P.J., 2006. The determination of the isotopic
1107 composition of Cu and Zn in seawater. Chem. Geol. 226, 280–297.
1108 https://doi.org/10.1016/j.chemgeo.2005.09.025

1109 Bigalke, M., Weyer, S., Kobza, J., Wilcke, W., 2010. Stable Cu and Zn isotope ratios as
1110 tracers of sources and transport of Cu and Zn in contaminated soil. Geochim.
1111 Cosmochim. Acta 74, 6801–6813. https://doi.org/10.1016/j.gca.2010.08.044

1112 Black, J.R., John, S.G., Kavner, A., 2014. Coupled effects of temperature and mass transport
1113 on the isotope fractionation of zinc during electroplating. Geochim. Cosmochim. Acta
1114 124, 272–282. https://doi.org/10.1016/j.gca.2013.09.016

1115 Black, J.R., Kavner, A., Schauble, E.A., 2011. Calculation of equilibrium stable isotope
1116 partition function ratios for aqueous zinc complexes and metallic zinc. Geochim.
1117 Cosmochim. Acta 75, 769–783. https://doi.org/10.1016/j.gca.2010.11.019

1118 Blau, P.J., 2001. Compositions , Functions , and Testing of Friction Brake Materials and
1119 Their Additives. Energy 27, 38. https://doi.org/http://dx.doi.org/10.2172/788356

1120 Borrok, D.M., Gieré, R., Ren, M., Landa, E.R., 2010. Zinc isotopic composition of particulate
1121 matter generated during the combustion of coal and coal + tire-derived fuels. Environ.

Sci. Technol. 44, 9219–9224. https://doi.org/10.1021/es102439g

Borrok, D.M., Nimick, D.A., Wanty, R.B., Ridley, W.I., 2008. Isotopic variations of dissolved copper and zinc in stream waters affected by historical mining. Geochim. Cosmochim. Acta 72, 329–344. https://doi.org/10.1016/j.gca.2007.11.014

Borrok, D.M., Wanty, R.B., Ridley, W.I., Lamothe, P.J., Kimball, B.A., Verplanck, P.L., Runkel, R.L., 2009. Application of iron and zinc isotopes to track the sources and mechanisms of metal loading in a mountain watershed. Appl. Geochemistry 24, 1270–1277. https://doi.org/10.1016/j.apgeochem.2009.03.010

Borrok, D.M., Wanty, R.B., Ridley, W.I., Wolf, R., Lamothe, P.J., Adams, M., 2007. Separation of copper, iron, and zinc from complex aqueous solutions for isotopic measurement. Chem. Geol. 242, 400–414. https://doi.org/10.1016/j.chemgeo.2007.04.004

Boyle, E.A., John, S., Abouchami, W., Adkins, J.F., Echegoyen-Sanz, Y., Ellwood, M., Flegal, A.R., Fornace, K., Gallon, C., Galer, S., Gault-Ringold, M., Lacan, F., Radic, A., Rehkamper, M., Rouxel, O., Sohrin, Y., Stirling, C., Thompson, C., Vance, D., Xue, Z., Zhao, Y., 2012. GEOTRACES IC1 (BATS) contamination-prone trace element isotopes Cd, Fe, Pb, Zn, Cu, and Mo intercalibration. Limnol. Oceanogr. 10, 653–665. https://doi.org/10.4319/lom.2012.10.653

Brassard, P., Hamelin, L., Singh, P., Godbout, S., 2012. Révision de l'AGDEX 538 / 400.27, rapport final.

Braun, M., Besozzi, D., Herata, H., Falcke, H., van Dokkum, R., Langenfeld, F., Mohaupt, V., van den Roovaart, J., Sieber, U., Sollberger, B., 2000. Rhin inventaire 2000 des émissions prioritaires. Rapport de la commission internationale pour la protection du Rhin.

Braxton, D., Mathur, R.D., 2011. Exploration applications of copper isotopes in the supergene environment: A case study of the bayugo porphyry copper-gold deposit, Southern Philippines. Econ. Geol. 106, 1447–1463.

Bryan, A.L., Dong, S., Wilkes, E.B., Wasylenki, L.E., 2015. Zinc isotope fractionation during adsorption onto Mn oxyhydroxide at low and high ionic strength. Geochim. Cosmochim. Acta 157, 182–197. https://doi.org/10.1016/j.gca.2015.01.026

Bullen, T., 2012. Stable isotopes of transition and post-transition metals as tracers in environmental studies., in: Handbook of Environmental Isotope Geochemistry. pp. 177–203. https://doi.org/10.1007/978-3-642-10637-8

Buzier, R., Tusseau-Vuillemin, M.H., dit Meriadec, C.M., Rousselot, O., Mouchel, J.M., 2006. Trace metal speciation and fluxes within a major French wastewater treatment plant: Impact of the successive treatments stages. Chemosphere 65, 2419–2426. https://doi.org/10.1016/j.chemosphere.2006.04.059

Caldelas, C., Dong, S., Araus, J.L., Weiss, D.J., 2011. Zinc isotopic fractionation in Phragmites australis in response to toxic levels of zinc. J. Exp. Bot. 62, 2169–2178. https://doi.org/10.1093/jxb/erq414

Campbell, P., 1995. Interactions between trace metals and aquatic organisms: a critique of the free-ion activity model, in: Tessier, A.; Turner, D.R. (Ed.), Metal Speciation and Bioavailability in Aquatic Systems. John Wiley and Sons, New York, NY.

Chaminda, G.G.T., Nakajima, F., Furumai, H., Kasuga, I., Kurisu, F., 2013. Metal (Zn, Cu, Cd and Ni) Complexation by Dissolved Organic Matter (DOM) in Wastewater Treatment Plant Effluent. J. Water Environ. Technol. 11, 153–161. https://doi.org/10.2965/jwet.2013.153

1169 Chapman, J.B., Mason, T.F.D., Weiss, D.J., Coles, B.J., Wilkinson, J.J., 2006. Chemical
1170 separation and isotopic variations of Cu and Zn from five geological reference materials.
1171 Geostand. Geoanalytical Res. 30, 5–16. https://doi.org/10.1111/j.1751-
1172 908X.2006.tb00907.x

1173 Chen, H., Savage, P.S., Teng, F.-Z., Helz, R.T., Moynier, F., 2013. Zinc isotope fractionation
1174 during magmatic differentiation and the isotopic composition of the bulk Earth. Earth
1175 Planet. Sci. Lett. 369–370, 34–42. https://doi.org/10.1016/J.EPSL.2013.02.037

1176 Chen, J., Gaillardet, J., Dessert, C., Villemant, B., Louvat, P., Crispi, O., Birck, J.L., Wang,
1177 Y.N., 2014. Zn isotope compositions of the thermal spring waters of La Soufrière
1178 volcano, Guadeloupe island. Geochim. Cosmochim. Acta 127, 67–82.
1179 https://doi.org/10.1016/j.gca.2013.11.022

1180 Chen, J., Gaillardet, J., Louvat, P., 2008. Zinc isotopes in the Seine River waters, France: A
1181 probe of anthropogenic contamination. Environ. Sci. Technol. 42, 6494–6501.
1182 https://doi.org/10.1021/es800725z

1183 Chen, J., Gaillardet, J., Louvat, P., Huon, S., 2009b. Zn isotopes in the suspended load of
1184 the Seine River, France: Isotopic variations and source determination. Geochim.
1185 Cosmochim. Acta 73, 4060–4076. https://doi.org/10.1016/j.gca.2009.04.017

1186 Chen, J., Louvat, P., Gaillardet, J., Birck, J.L., 2009a. Direct separation of Zn from dilute
1187 aqueous solutions for isotope composition determination using multi-collector ICP-MS.
1188 Chem. Geol. 259, 120–130. https://doi.org/10.1016/j.chemgeo.2008.10.040

1189 Chen, S., Liu, Y., Hu, J., Zhang, Z., Hou, Z., Huang, F., Yu, H., 2016. Zinc Isotopic
1190 Compositions of NIST SRM 683 and Whole-Rock Reference Materials. Geostand.
1191 Geoanalytical Res. 40, 417–432. https://doi.org/10.1111/j.1751-908X.2015.00377.x

1192 Cloquet, C., Carignan, J., Lehmann, M.F., Vanhaecke, F., 2008. Variation in the isotopic
1193 composition of zinc in the natural environment and the use of zinc isotopes in
1194 biogeosciences: A review. Anal. Bioanal. Chem. https://doi.org/10.1007/s00216-007-
1195 1635-y

1196 Cloquet, C., Carignan, J., Libourel, G., 2006. Isotopic composition of Zn and Pb atmospheric
1197 depositions in an urban/periurban area of northeastern France. Environ. Sci. Technol.
1198 40, 6594–6600. https://doi.org/10.1021/es0609654

1199 Couder, E.., Delvaux, B.., Maerschalk, C.., Mattielli, N., 2008. Zinc isotopes in polluted
1200 substrates The influence of phase separation on the flow patterns of mid-ocean ridge
1201 hydrothermal systems. Geochim. Cosmochim. Acta 72, A184.

1202 Couder, E., Mattielli, N., Drouet, T., Smolders, E., Delvaux, B., Iserentant, A., Meeus, C.,
1203 Maerschalk, C., Opfergelt, S., Houben, D., 2015. Transpiration flow controls Zn
1204 transport in Brassica napus and Lolium multiflorum under toxic levels as evidenced from
1205 isotopic fractionation. Comptes Rendus - Geosci. 347, 386–396.
1206 https://doi.org/10.1016/j.crte.2015.05.004

1207 Councell, T.B., Duckenfield, K.U., Landa, E.R., Callender, E., 2004. Tire-wear particles as a
1208 source of zinc to the environment. Environ. Sci. Technol. 38, 4206–4214.
1209 https://doi.org/10.1021/es034631f

1210 Coutaud, A., Meheut, M., Viers, J., Rols, J.L., Pokrovsky, O.S., 2014. Zn isotope fractionation
1211 during interaction with phototrophic biofilm. Chem. Geol. 390, 46–60.
1212 https://doi.org/10.1016/j.chemgeo.2014.10.004

1213 da Rosa Couto, R., Benedet, L., Comin, J.J., Filho, P.B., Martins, S.R., Gatiboni, L.C.,
1214 Radetski, M., de Valois, C.M., Ambrosini, V.G., Brunetto, G., 2015. Accumulation of
1215 copper and zinc fractions in vineyard soil in the mid-western region of Santa Catarina,

Brazil. Environ. Earth Sci. 73, 6379–6386. https://doi.org/10.1007/s12665-014-3861-x

Deng, J., Wang, C., Bagas, L., Selvaraja, V., Jeon, H., Wu, B., Yang, L., 2017. Insights into ore genesis of the Jinding Zn–Pb deposit, Yunnan Province, China: Evidence from Zn and in-situ S isotopes. Ore Geol. Rev. 90, 943–957. https://doi.org/10.1016/j.oregeorev.2016.10.036

Desaulty, A.-M., Méheut, M., Guerrot, C., Berho, C., Millot, R., 2017. Coupling DGT passive samplers and multi-collector ICP-MS: A new tool to measure Pb and Zn isotopes composition in dilute aqueous solutions. Chem. Geol. 450, 122–134. https://doi.org/10.1016/j.chemgeo.2016.12.023

Desaulty, A.-M., Millot, R., 2017. Projet ISOP2 : Origine, mobilité et répartition eaux/sédiments des métaux (Pb, Zn, Cu) : exemple de deux sous-bassins versants (Argos et Egoutier) du bassin Loire-Bretagne. Rapport BRGM, RP-66799-FR.

Dong, S., Ochoa Gonzalez, R., Harrison, R.M., Green, D., North, R., Fowler, G., Weiss, D., 2017. Isotopic signatures suggest important contributions from recycled gasoline, road dust and non-exhaust traffic sources for copper, zinc and lead in PM10 in London, United Kingdom. Atmos. Environ. 165, 88–98. https://doi.org/10.1016/j.atmosenv.2017.06.020

Dong, S., Wasylenki, L.E., 2016. Zinc isotope fractionation during adsorption to calcite at high and low ionic strength. Geochim. Cosmochim. Acta 157, 182–197. https://doi.org/10.1016/j.gca.2015.01.026

Duan, J., Tang, J., Lin, B., 2016. Zinc and lead isotope signatures of the Zhaxikang Pb-Zn deposit, South Tibet: Implications for the source of the ore-forming metals. Ore Geol. Rev. 78, 58–68. https://doi.org/10.1016/j.oregeorev.2016.03.019

Ducher, M., Blanchard, M., Balan, E., 2018. Equilibrium isotopic fractionation between aqueous Zn and minerals from first-principles calculations. Chem. Geol. 483, 342–350. https://doi.org/10.1016/j.chemgeo.2018.02.040

Ducher, M., Blanchard, M., Balan, E., 2016. Equilibrium zinc isotope fractionation in Zn-bearing minerals from first-principles calculations. Chem. Geol. 443, 87–96. https://doi.org/10.1016/j.chemgeo.2016.09.016

Duplay, J., Semhi, K., Errais, E., Imfeld, G., Babcsanyi, I., Perrone, T., 2014. Copper, zinc, lead and cadmium bioavailability and retention in vineyard soils (Rouffach, France): The impact of cultural practices. Geoderma 230–231, 318–328. https://doi.org/10.1016/j.geoderma.2014.04.022

Eriksson, J., 2001. Concentrations of 61 trace elements in sewage sludge, farmyard manure, mineral fertiliser, precipitation and in oil and crops, Swedish Environmental Protection Agency, Stockholm, Sweden.

Fekiacova, Z., Cornu, S., Pichat, S., 2015. Tracing contamination sources in soils with Cu and Zn isotopic ratios. Sci. Total Environ. 517, 96–105. https://doi.org/10.1016/j.scitotenv.2015.02.046

Fernandez, A., Borrok, D.M., 2009. Fractionation of Cu, Fe, and Zn isotopes during the oxidative weathering of sulfide-rich rocks. Chem. Geol. 264, 1–12. https://doi.org/10.1016/j.chemgeo.2009.01.024

Fujii, T., Albarède, F., 2012. Ab initio calculation of the Zn isotope effect in phosphates, citrates, and malates and applications to plants and soil. PLoS One 7. https://doi.org/10.1371/journal.pone.0030726

Fujii, T., Moynier, F., Blichert-Toft, J., Albarède, F., 2014. Density functional theory

1262 estimation of isotope fractionation of Fe, Ni, Cu, and Zn among species relevant to
1263 geochemical and biological environments. Geochim. Cosmochim. Acta 140, 553–576.
1264 https://doi.org/10.1016/j.gca.2014.05.051

1265 Fujii, T., Moynier, F., Pons, M.L., Albarède, F., 2011. The origin of Zn isotope fractionation in
1266 sulfides. Geochim. Cosmochim. Acta 75, 7632–7643.
1267 https://doi.org/10.1016/j.gca.2011.09.036

1268 Fujii, T., Moynier, F., Telouk, P., Abe, M., 2010. Experimental and theoretical investigation of
1269 isotope fractionation of zinc between aqua, chloro, and macrocyclic complexes. J. Phys.
1270 Chem. A 114, 2543–2552. https://doi.org/10.1021/jp908642f

1271 Gagnevin, D., Boyce, A.J., Barrie, C.D., Menuge, J.F., Blakeman, R.J., 2012. Zn, Fe and S
1272 isotope fractionation in a large hydrothermal system. Geochim. Cosmochim. Acta 88,
1273 183–198. https://doi.org/10.1016/j.gca.2012.04.031

1274 Gaillardet, J., Viers, J., Dupré, B., 2003. Trace elements in river waters, in: Heinrich, D. H.;
1275 Karl, K.T. (Ed.), Treatise on Geochemistry. Oxford, pp. 225–272.
1276 https://doi.org/10.1021/es0629920

1277 Gélabert, A., Pokrovsky, O.S., Viers, J., Schott, J., Boudou, A., Feurtet-Mazel, A., 2006.
1278 Interaction between zinc and freshwater and marine diatom species: Surface
1279 complexation and Zn isotope fractionation. Geochim. Cosmochim. Acta 70, 839–857.
1280 https://doi.org/10.1016/j.gca.2005.10.026

1281 Gelly, R., Fekiacova, Z., Guihou, A., Doelsch, E., Deschamps, P., Keller, C., 2019. Lead,
1282 zinc, and copper redistributions in soils along a deposition gradient from emissions of a
1283 Pb-Ag smelter decommissioned 100 years ago. Sci. Total Environ. 665, 502–512.
1284 https://doi.org/10.1016/j.scitotenv.2019.02.092

1285 Gioia, S., Weiss, D., Coles, B., Arnold, T., Babinski, M., 2008. Accurate and precise zinc
1286 isotope ratio measurements in urban aerosols. Anal. Chem. 80, 9776–9780.
1287 https://doi.org/10.1021/ac8019587

1288 Gordon, R.B., Graedel, T.E., Bertram, M., Fuse, K., Lifset, R., Rechberger, H., Spatari, S.,
1289 2003. The characterization of technological zinc cycles. Resour. Conserv. Recycl. 39,
1290 107–135. https://doi.org/10.1016/S0921-3449(02)00166-0

1291 Gou, W., Li, W., Ji, J., Li, W., 2018. Zinc Isotope Fractionation during Sorption onto Al
1292 Oxides: Atomic Level Understanding from EXAFS. Environ. Sci. Technol. 52, 9087–
1293 9096. https://doi.org/10.1021/acs.est.8b01414

1294 Gourlay-Francé, C., Bressy, A., Uher, E., Lorgeoux, C., 2011. Labile, dissolved and
1295 particulate PAHs and trace metals in wastewater: Passive sampling, occurrence,
1296 partitioning in treatment plants. Water Sci. Technol. 63, 1327–1333.
1297 https://doi.org/10.2166/wst.2011.127

1298 Gouzy, A., Brignon, J.-M., 2014. Données technico-économiques sur les substances
1299 chimiques en France : Zinc et principaux composés. Rapport INERIS, DRC-14-136881-
1300 02237A.

1301 Guinoiseau, D., Bouchez, J., Gélabert, A., Louvat, P., Moreira-Turcq, P., Filizola, N.,
1302 Benedetti, M.F., 2018. Fate of particulate copper and zinc isotopes at the Solimões-
1303 Negro river confluence, Amazon Basin, Brazil. Chem. Geol. 489, 1–15.
1304 https://doi.org/10.1016/j.chemgeo.2018.05.004

1305 Guinoiseau, D., Gélabert, A., Allard, T., Louvat, P., Moreira-Turcq, P., Benedetti, M.F., 2017.
1306 Zinc and copper behaviour at the soil-river interface: New insights by Zn and Cu
1307 isotopes in the organic-rich Rio Negro basin. Geochim. Cosmochim. Acta 213, 178–197.
1308 https://doi.org/10.1016/j.gca.2017.06.030

1309 Guinoiseau, D., Gélabert, A., Moureau, J., Louvat, P., Benedetti, M.F., 2016. Zn isotope
1310 fractionation during sorption onto kaolinite. Environ. Sci. Technol. 50, 1844–1852.
1311 https://doi.org/10.1021/acs.est.5b05347

1312 Hjortenkrans, D.S.T., Bergbäck, B.G., Häggerud, A. V., 2007. Metal emissions from brake
1313 linings and tires: Case studies of Stockholm, Sweden 1995/1998 and 2005. Environ.
1314 Sci. Technol. 41, 5224–5230. https://doi.org/10.1021/es070198o

1315 Houben, D., Sonnet, P., Tricot, G., Mattielli, N., Couder, E., Opfergelt, S., 2014. Impact of
1316 root-induced mobilization of zinc on stable Zn isotope variation in the soil-plant system.
1317 Environ. Sci. Technol. 48, 7866–7873. https://doi.org/10.1021/es5002874

1318 Jamieson-Hanes, J.H., Shrimpton, H.K., Veeramani, H., Ptacek, C.J., Lanzirotti, A., Newville,
1319 M., Blowes, D.W., 2017. Evaluating zinc isotope fractionation under sulfate reducing
1320 conditions using a flow-through cell and in situ XAS analysis. Geochim. Cosmochim.
1321 Acta 203, 1–14. https://doi.org/10.1016/j.gca.2016.12.034

1322 John, S.G., Conway, T.M., 2014. A role for scavenging in the marine biogeochemical cycling
1323 of zinc and zinc isotopes. Earth Planet. Sci. Lett. 394, 159–167.
1324 https://doi.org/10.1016/j.epsl.2014.02.053

1325 John, S.G., Geis, R.W., Saito, M.A., Boyle, E.A., 2007a. Zinc isotope fractionation during
1326 high-affinity and low-affinity zinc transport by the marine diatom Thalassiosira oceanica.
1327 Limnol. Oceanogr. 52, 2710–2714. https://doi.org/10.4319/lo.2007.52.6.2710

1328 John, S.G., Genevieve Park, J., Zhang, Z., Boyle, E.A., 2007b. The isotopic composition of
1329 some common forms of anthropogenic zinc. Chem. Geol. 245, 61–69.
1330 https://doi.org/10.1016/j.chemgeo.2007.07.024

1331 John, S.G., Rouxel, O.J., Craddock, P.R., Engwall, A.M., Boyle, E.A., 2008. Zinc stable
1332 isotopes in seafloor hydrothermal vent fluids and chimneys. Earth Planet. Sci. Lett. 269,
1333 17–28. https://doi.org/10.1016/j.epsl.2007.12.011

1334 Jouvin, D., Louvat, P., Juillot, F., Maréchal, C.N., Benedetti, M.F., 2009. Zinc Isotopic
1335 Fractionation: Why Organic Matters. Environ. Sci. Technol. 43, 5747–5754.
1336 https://doi.org/10.1021/es803012e

1337 Jouvin, D., Weiss, D.J., Mason, T.F.M., Bravin, M.N., Louvat, P., Zhao, F., Ferec, F.,
1338 Hinsinger, P., Benedetti, M.F., 2012. Stable isotopes of Cu and Zn in higher plants:
1339 Evidence for Cu reduction at the root surface and two conceptual models for isotopic
1340 fractionation processes. Environ. Sci. Technol. 46, 2652–2660.
1341 https://doi.org/10.1021/es202587m

1342 Juillot, F., Maréchal, C., Morin, G., Jouvin, D., Cacaly, S., Telouk, P., Benedetti, M.F.,
1343 Ildefonse, P., Sutton, S., Guyot, F., Brown, G.E., 2011. Contrasting isotopic signatures
1344 between anthropogenic and geogenic Zn and evidence for post-depositional
1345 fractionation processes in smelter-impacted soils from Northern France. Geochim.
1346 Cosmochim. Acta 75, 2295–2308. https://doi.org/10.1016/j.gca.2011.02.004

1347 Juillot, F., Maréchal, C., Ponthieu, M., Cacaly, S., Morin, G., Benedetti, M., Hazemann, J.L.,
1348 Proux, O., Guyot, F., 2008. Zn isotopic fractionation caused by sorption on goethite and
1349 2-Lines ferrihydrite. Geochim. Cosmochim. Acta 72, 4886–4900.
1350 https://doi.org/10.1016/j.gca.2008.07.007

1351 Kafantaris, F.C.A., Borrok, D.M., 2014. Zinc isotope fractionation during surface adsorption
1352 and intracellular incorporation by bacteria. Chem. Geol. 366, 42–51.
1353 https://doi.org/10.1016/j.chemgeo.2013.12.007

1354 Kavner, A., John, S.G., Sass, S., Boyle, E.A., 2008. Redox-driven stable isotope fractionation
1355 in transition metals: Application to Zn electroplating. Geochim. Cosmochim. Acta 72,

1731–1741. https://doi.org/10.1016/j.gca.2008.01.023

Kelley, K.D.., Wilkinson, J.J.., Chapman, J.B.., Crowther, H.L.., Weiss, D.J., 2009. Zinc isotopes in sphalerite from base metal deposits in the Red Dog District, Northern Alaska. Econ. Geol. 104, 767–773.

Kos Durjava, M., Kolar, B., Balk, F., Peijnenburg, W., 2015. Water Framework Directive and Specific Pollutants in Surface Waters in Slovenia. Acta hydrotechnica 45, 61–69.

Legret, M., Pagotto, C., 1999. Evaluation of pollutant loadings in the runoff waters from a major rural highway, in: Science of the Total Environment. pp. 143–150. https://doi.org/10.1016/S0048-9697(99)00207-7

Levasseur, P., 2005. Teneur en cuivre et zinc des lisiers et des fumiers de porcs charcutiers après réduction de leur concentration dans les aliments après réduction de leur concentration dans les aliments. Tech. Porc Vol. 28, N, 21–24.

Levasseur, P., Texier, C., 2001. Teneurs en éléments-trace métalliques des aliments et des lisiers de porcs à l'engrais, de truies et de porcelets. Journées Rech. Porc. en Fr. 33, 57–62.

Little, S.H., Vance, D., Walker-Brown, C., Landing, W.M., 2014. The oceanic mass balance of copper and zinc isotopes, investigated by analysis of their inputs, and outputs to ferromanganese oxide sediments. Geochim. Cosmochim. Acta 125, 673–693. https://doi.org/10.1016/j.gca.2013.07.046

Maréchal, C.N., Télouk, P., Albarède, F., 1999. Precise analysis of copper and zinc isotopic compositions by plasma-source mass spectrometry. Chem. Geol. 156, 251–273. https://doi.org/10.1016/S0009-2541(98)00191-0

Martin, J.-M., Meybeck, M., 1979. Elemental mass-balance of material carried by major world rivers. Mar. Chem. 7, 173–206. https://doi.org/10.1016/0304-4203(79)90039-2

Mason, T.F.D., Weiss, D.J., Chapman, J.B., Wilkinson, J.J., Tessalina, S.G., Spiro, B., Horstwood, M.S.A., Spratt, J., Coles, B.J., 2005. Zn and Cu isotopic variability in the Alexandrinka volcanic-hosted massive sulphide (VHMS) ore deposit, Urals, Russia. Chem. Geol. 221, 170–187. https://doi.org/10.1016/j.chemgeo.2005.04.011

Mattielli, N., Petit, J.C.J., Deboudt, K., Flament, P., Perdrix, E., Taillez, A., Rimetz-Planchon, J., Weis, D., 2009. Zn isotope study of atmospheric emissions and dry depositions within a 5 km radius of a Pb–Zn refinery. Atmos. Environ. 43, 1265–1272. https://doi.org/10.1016/j.atmosenv.2008.11.030

Meeddat, 2009. Eléments de contexte et réglementation française relatifs à la valorisation des boues issues du traitement des eaux usées, Meeddat note.

Moeller, K., Schoenberg, R., Pedersen, R.B., Weiss, D., Dong, S., 2012. Calibration of the New Certified Reference Materials ERM-AE633 and ERM-AE647 for Copper and IRMM-3702 for Zinc Isotope Amount Ratio Determinations. Geostand. Geoanalytical Res. 36, 177–199. https://doi.org/10.1111/j.1751-908X.2011.00153.x

Mondillo, N., Wilkinson, J.J., Boni, M., Weiss, D.J., Mathur, R., 2018. A global assessment of Zn isotope fractionation in secondary Zn minerals from sulfide and non-sulfide ore deposits and model for fractionation control. Chem. Geol. 500, 182–193. https://doi.org/10.1016/j.chemgeo.2018.09.033

Montgomery, J.R., Santiago, R.J., 1978. Zinc and copper in "particulate" forms and "soluble" complexes with inorganic or organic ligands in the guanajibo river and coastal zone, Puerto Rico. Estuar. Coast. Mar. Sci. 6, 111–116. https://doi.org/10.1016/0302-3524(78)90046-4

1402 Moynier, F., Vance, D., Fujii, T., Savage, P., 2017. The Isotope Geochemistry of Zinc and
1403 Copper. Rev. Mineral. Geochemistry 82, 543–600.
1404 https://doi.org/10.2138/rmg.2017.82.13

1405 Muyssen, B.T.A., De Schamphelaere, K.A.C., Janssen, C.R., 2006. Mechanisms of chronic
1406 waterborne Zn toxicity in Daphnia magna. Aquat. Toxicol. 77, 393–401.
1407 https://doi.org/10.1016/j.aquatox.2006.01.006

1408 Nelson, J., Wasylenki, L., Bargar, J.R., Brown, G.E., Maher, K., 2017. Effects of surface
1409 structural disorder and surface coverage on isotopic fractionation during Zn(II)
1410 adsorption onto quartz and amorphous silica surfaces. Geochim. Cosmochim. Acta 215,
1411 354–376. https://doi.org/10.1016/j.gca.2017.08.003

1412 Nicholson, F.A., Chambers, B.J., Williams, J.R., Unwin, R.J., 1999. Heavy metal contents of
1413 livestock feeds and animal manures in England and Wales. Bioresour. Technol. 70, 23–
1414 31. https://doi.org/10.1016/S0960-8524(99)00017-6

1415 Nomngongo, P.N., Ngila, J.C., 2014. Determination of trace Cd, Cu, Fe, Pb and Zn in diesel
1416 and gasoline by inductively coupled plasma mass spectrometry after sample clean up
1417 with hollow fiber solid phase microextraction system. Spectrochim. Acta - Part B At.
1418 Spectrosc. 98, 54–59. https://doi.org/10.1016/j.sab.2014.06.001

1419 Novak, M., Sipkova, A., Chrastny, V., Stepanova, M., Voldrichova, P., Veselovsky, F.,
1420 Prechova, E., Blaha, V., Curik, J., Farkas, J., Erbanova, L., Bohdalkova, L., Pasava, J.,
1421 Mikova, J., Komarek, A., Krachler, M., 2016. Cu-Zn isotope constraints on the
1422 provenance of air pollution in Central Europe: Using soluble and insoluble particles in
1423 snow and rime. Environ. Pollut. 218, 1135–1146.
1424 https://doi.org/10.1016/j.envpol.2016.08.067

1425 Nriagu, J.O., Pacyna, J.M., 1988. Quantitative assessment of worldwide contamination of air,
1426 water and soils by trace metals. Nature 333, 134–139. https://doi.org/10.1038/333134a0

1427 Ochoa Gonzalez, R., Weiss, D., 2015. Zinc Isotope Variability in Three Coal-Fired Power
1428 Plants: A Predictive Model for Determining Isotopic Fractionation during Combustion.
1429 Environ. Sci. Technol. 49, 12560–12567. https://doi.org/10.1021/acs.est.5b02402

1430 Pašava, J., Tornos, F., Chrastný, V., 2014. Zinc and sulfur isotope variation in sphalerite
1431 from carbonate-hosted zinc deposits, Cantabria, Spain. Miner. Depos. 49, 797–807.
1432 https://doi.org/10.1007/s00126-014-0535-2

1433 Petit, J.C.J., de Jong, J., Chou, L., Mattielli, N., 2008. Development of Cu and Zn isotope
1434 MC-ICP-MS measurements: Application to suspended particulate matter and sediments
1435 from the scheldt estuary. Geostand. Geoanalytical Res. 32, 149–166.
1436 https://doi.org/10.1111/j.1751-908X.2008.00867.x

1437 Petit, J.C.J., Schäfer, J., Coynel, A., Blanc, G., Chiffoleau, J.F., Auger, D., Bossy, C.,
1438 Derriennic, H., Mikolaczyk, M., Dutruch, L., Mattielli, N., 2015. The estuarine
1439 geochemical reactivity of Zn isotopes and its relevance for the biomonitoring of
1440 anthropogenic Zn and Cd contaminations from metallurgical activities: Example of the
1441 Gironde fluvial-estuarine system, France. Geochim. Cosmochim. Acta 170, 108–125.
1442 https://doi.org/10.1016/j.gca.2015.08.004

1443 Pokrovsky, O.S., Viers, J., Freydier, R., 2005. Zinc stable isotope fractionation during its
1444 adsorption on oxides and hydroxides. J. Colloid Interface Sci. 291, 192–200.
1445 https://doi.org/10.1016/j.jcis.2005.04.079

1446 Rosman, K.J.R., 1972. A survey of the isotopic and elemental abundance of zinc. Geochim.
1447 Cosmochim. Acta 36, 801–819. https://doi.org/10.1016/0016-7037(72)90089-0

1448 Samanta, M., Ellwood, M.J., Strzepek, R.F., 2018. Zinc isotope fractionation by Emiliania

huxleyi cultured across a range of free zinc ion concentrations. Limnol. Oceanogr. 63, 660–671. https://doi.org/10.1002/lno.10658

Schauble, E.A., 2004. Applying stable isotope fractionation theory to new systems. Rev. Mineral. Geochemistry 55, 65–111. https://doi.org/10.2138/gsrmg.55.1.65

Schmidt, T.S., Clements, W.H., Zuellig, R.E., Mitchell, K.A., Church, S.E., Wanty, R.B., San Juan, C.A., Adams, M., Lamothe, P.J., 2011. Critical tissue residue approach linking accumulated metals in aquatic insects to population and community-level effects. Environ. Sci. Technol. 45, 7004–7010. https://doi.org/10.1021/es200215s

Schoenberg, R., Von Blanckenburg, F., 2005. An assessment of the accuracy of stable Fe isotope ratio measurements on samples with organic and inorganic matrices by high-resolution multicollector ICP-MS. Int. J. Mass Spectrom. 242, 257–272. https://doi.org/10.1016/j.ijms.2004.11.025

Schönbächler, M., Carlson, R.W., Horan, M.F., Mock, T.D., Hauri, E.H., 2007. High precision Ag isotope measurements in geologic materials by multiple-collector ICPMS: An evaluation of dry versus wet plasma. Int. J. Mass Spectrom. 261, 183–191. https://doi.org/10.1016/j.ijms.2006.09.016

Shiel, A.E., Weis, D., Orians, K.J., 2010. Evaluation of zinc, cadmium and lead isotope fractionation during smelting and refining. Sci. Total Environ. 408, 2357–2368. https://doi.org/10.1016/j.scitotenv.2010.02.016

Sivry, Y., Riotte, J., Sonke, J.E., Audry, S., Schäfer, J., Viers, J., Blanc, G., Freydier, R., Dupré, B., 2008. Zn isotopes as tracers of anthropogenic pollution from Zn-ore smelters The Riou Mort-Lot River system. Chem. Geol. 255, 295–304. https://doi.org/10.1016/j.chemgeo.2008.06.038

Skierszkan, E.K., Mayer, K.U., Weis, D., Beckie, R.D., 2016. Molybdenum and zinc stable isotope variation in mining waste rock drainage and waste rock at the Antamina mine, Peru. Sci. Total Environ. 550, 103–113. https://doi.org/10.1016/j.scitotenv.2016.01.053

Smith, W.H., Plumlee, M.P., Beeson, W.M., 1962. Effect of source of protein on zinc requirement of the growing pig. J. Anim. Sci. 21, 399–405. https://doi.org/10.2527/jas1962.213399x

Smolders, E., Versieren, L., Shuofei, D., Mattielli, N., Weiss, D., Petrov, I., Degryse, F., 2013. Isotopic fractionation of Zn in tomato plants suggests the role of root exudates on Zn uptake. Plant Soil 370, 605–613. https://doi.org/10.1007/s11104-013-1655-7

Sonke, J.E., Sivry, Y., Viers, J., Freydier, R., Dejonghe, L., André, L., Aggarwal, J.K., Fontan, F., Dupré, B., 2008. Historical variations in the isotopic composition of atmospheric zinc deposition from a zinc smelter. Chem. Geol. 252, 145–157. https://doi.org/10.1016/j.chemgeo.2008.02.006

Souto-Oliveira, C.E., Babinski, M., Araújo, D.F., Andrade, M.F., 2018. Multi-isotopic fingerprints (Pb, Zn, Cu) applied for urban aerosol source apportionment and discrimination. Sci. Total Environ. 626, 1350–1366. https://doi.org/10.1016/j.scitotenv.2018.01.192

Souto-Oliveira, C.E., Babinski, M., Araújo, D.F., Weiss, D.J., Ruiz, I.R., 2019. Multi-isotope approach of Pb, Cu and Zn in urban aerosols and anthropogenic sources improves tracing of the atmospheric pollutant sources in megacities. Atmos. Environ. 198, 427–437. https://doi.org/10.1016/j.atmosenv.2018.11.007

Szynkiewicz, A., Borrok, D.M., 2016. Isotope variations of dissolved Zn in the Rio Grande watershed, USA: The role of adsorption on Zn isotope composition. Earth Planet. Sci. Lett. 433, 293–302. https://doi.org/10.1016/j.epsl.2015.10.050

1496 Tang, Y.T., Cloquet, C., Deng, T.H.B., Sterckeman, T., Echevarria, G., Yang, W.J., Morel,
1497 J.L., Qiu, R.L., 2016. Zinc Isotope Fractionation in the Hyperaccumulator Noccaea
1498 caerulescens and the Nonaccumulating Plant Thlaspi arvense at Low and High Zn
1499 Supply. Environ. Sci. Technol. 50, 8020–8027. https://doi.org/10.1021/acs.est.6b00167

1500 Taylor, S., McLennan, S., 1985. The continental crust: its composition and evolution,
1501 Blackwell. Oxford. https://doi.org/10.1126/science.209.4452.96

1502 Thapalia, A., Borrok, D.M., Van Metre, P.C., Musgrove, M., Landa, E.R., 2010. Zn and Cu
1503 isotopes as tracers of anthropogenic contamination in a sediment core from an Urban
1504 Lake. Environ. Sci. Technol. 44, 1544–1550. https://doi.org/10.1021/es902933y

1505 Thapalia, A., Borrok, D.M., Van Metre, P.C., Wilson, J., 2015. Zinc isotopic signatures in
1506 eight lake sediment cores from across the United States. Environ. Sci. Technol. 49,
1507 132–40. https://doi.org/10.1021/es5036893

1508 United States Environmental Protection Agency, 1996. 1995 Updates: Water Quality Criteria
1509 Documents for the Protection of Aquatic Life in Ambient Water, EPA 820-B-96-001.

1510 van den Berg, C.M.G., Dharmvanij, S., 1984. Organic complexation of zinc in estuarine
1511 interstitial and surface water samples. Limnol. Oceanogr. 29, 1025–1036.
1512 https://doi.org/10.4319/lo.1984.29.5.1025

1513 Vance, D., Matthews, A., Keech, A., Archer, C., Hudson, G., Pett-Ridge, J., Chadwick, O.A.,
1514 2016. The behaviour of Cu and Zn isotopes during soil development: Controls on the
1515 dissolved load of rivers. Chem. Geol. 445, 36–53.
1516 https://doi.org/10.1016/j.chemgeo.2016.06.002

1517 Veeramani, H., Eagling, J., Jamieson-Hanes, J.H., Kong, L., Ptacek, C.J., Blowes, D.W.,
1518 2015. Zinc isotope fractionation as an indicator of geochemical attenuation processes.
1519 Environ. Sci. Technol. Lett. 2, 314–319. https://doi.org/10.1021/acs.estlett.5b00273

1520 Viers, J., Dupré, B., Gaillardet, J., 2009. Chemical composition of suspended sediments in
1521 World Rivers: New insights from a new database. Sci. Total Environ. 407, 853–868.
1522 https://doi.org/10.1016/j.scitotenv.2008.09.053

1523 Viers, J., Oliva, P., Nonell, A., Gélabert, A., Sonke, J.E., Freydier, R., Gainville, R., Dupré, B.,
1524 2007. Evidence of Zn isotopic fractionation in a soil-plant system of a pristine tropical
1525 watershed (Nsimi, Cameroon). Chem. Geol. 239, 124–137.
1526 https://doi.org/10.1016/j.chemgeo.2007.01.005

1527 Voldrichova, P., Chrastny, V., Sipkova, A., Farkas, J., Novak, M., Stepanova, M., Krachler,
1528 M., Veselovsky, F., Blaha, V., Prechova, E., Komarek, A., Bohdalkova, L., Curik, J.,
1529 Mikova, J., Erbanova, L., Pacherova, P., 2014. Zinc isotope systematics in snow and ice
1530 accretions in Central European mountains. Chem. Geol. 388, 130–141.
1531 https://doi.org/10.1016/j.chemgeo.2014.09.008

1532 Walsh, C.T., Sandstead, H.H., Prasad, A.S., Newberne, P.M., Fraker, P.J., 1994. Zinc:
1533 Health effects and research priorities for the 1990s. Environ. Health Perspect.
1534 https://doi.org/10.1289/ehp.941025

1535 Wanty, R.B., Podda, F., De Giudici, G., Cidu, R., Lattanzi, P., 2013. Zinc isotope and
1536 transition-element dynamics accompanying hydrozincite biomineralization in the Rio
1537 Naracauli, Sardinia, Italy. Chem. Geol. 337–338, 1–10.
1538 https://doi.org/10.1016/j.chemgeo.2012.11.010

1539 Weiss, D.J., Mason, T.F.D., Zhao, F.J., Kirk, G.J.D., Coles, B.J., Horstwood, M.S.A., 2005.
1540 Isotopic discrimination of zinc in higher plants. New Phytol. 165, 703–710.
1541 https://doi.org/10.1111/j.1469-8137.2004.01307.x

Weiss, D.J., Rausch, N., Mason, T.F.D., Coles, B.J., Wilkinson, J.J., Ukonmaanaho, L., Arnold, T., Nieminen, T.M., 2007. Atmospheric deposition and isotope biogeochemistry of zinc in ombrotrophic peat. Geochim. Cosmochim. Acta 71, 3498–3517. https://doi.org/10.1016/j.gca.2007.04.026

Whitton, B.A., 1970. Toxicity of heavy metals to freshwater algae: a review. Phykos 9, 116–125.

Wiederhold, J.G., 2015. Metal stable isotope signatures as tracers in environmental geochemistry. Environ. Sci. Technol. 49, 2606–2624. https://doi.org/10.1021/es504683e

Wilkinson, J.J., Weiss, D.J., Mason, T.F.D., Coles, B.J., 2005. Zinc isotope variation in hydrothermal systems: Preliminary evidence from the Irish Midlands ore field. Econ. Geol. 100, 583–590.

Xu, M., Yan, R., Zheng, C., Qiao, Y., Han, J., Sheng, C., 2004. Status of trace element emission in a coal combustion process: A review. Fuel Process. Technol. https://doi.org/10.1016/S0378-3820(03)00174-7

Yang, Y., Zhang, X., Liu, S.A., Zhou, T., Fan, H., Yu, H., Cheng, W., Huang, F., 2018. Calibrating NIST SRM 683 as a new international reference standard for Zn isotopes. J. Anal. At. Spectrom. 33, 1777–1783. https://doi.org/10.1039/c8ja00249e

Yin, N.H., Sivry, Y., Benedetti, M.F., Lens, P.N.L., van Hullebusch, E.D., 2015. Application of Zn isotopes in environmental impact assessment of Zn-Pb metallurgical industries: A mini review. Appl. Geochemistry 64, 128–135. https://doi.org/10.1016/j.apgeochem.2015.09.016

Yin, N.H., van Hullebusch, E.D., Benedetti, M., Lens, P.N.L., Sivry, Y., 2018. Zn isotopes fractionation during slags' weathering: One source of contamination, multiple isotopic signatures. Chemosphere 195, 483–490. https://doi.org/10.1016/j.chemosphere.2017.11.184

Zarcinas, B.A., Rogers, S.L., 2002. Copper, lead and zinc mobility and bioavailability in a river sediment contaminated with paint stripping residue. Environ. Geochem. Health 24, 191–203.

Zhao, Y., Vance, D., Abouchami, W., de Baar, H.J.W., 2014. Biogeochemical cycling of zinc and its isotopes in the Southern Ocean. Geochim. Cosmochim. Acta 125, 653–672. https://doi.org/10.1016/j.gca.2013.07.045

Zhou, J.X., Huang, Z.L., Zhou, M.F., Zhu, X.K., Muchez, P., 2014. Zinc, sulfur and lead isotopic variations in carbonate-hosted Pb-Zn sulfide deposits, southwest China. Ore Geol. Rev. 58, 41–54. https://doi.org/10.1016/j.oregeorev.2013.10.009

Figures

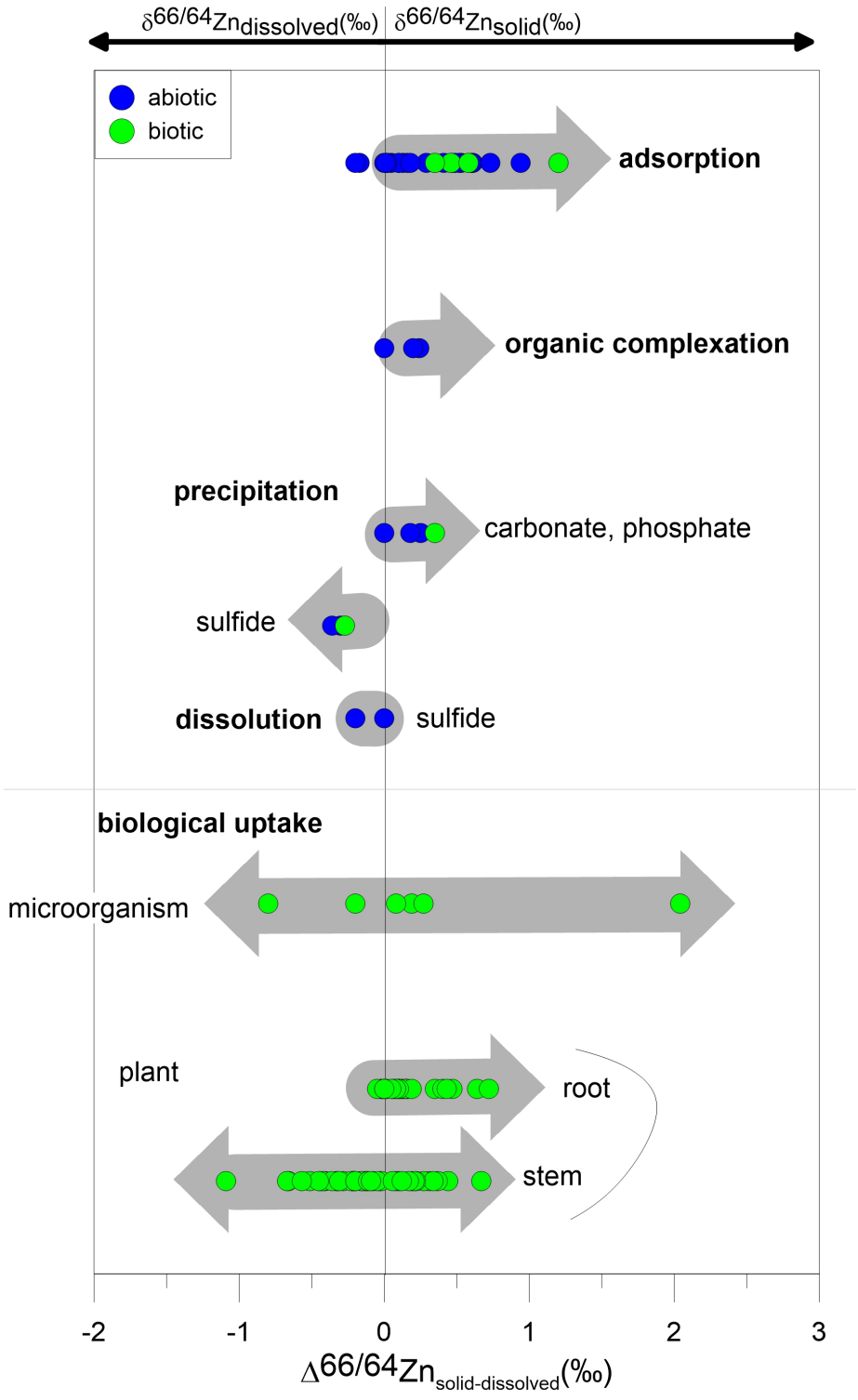

Fig. 1. Summary of the main physical and chemical processes altering the isotope compositions of zinc in the environment: adsorption onto mineral particles and biological surfaces, organic complexation, mineral phase precipitation/dissolution, zinc medium uptake by microorganisms and plants (Archer et al., 2004; Arnold et al., 2015, 2010b; Aucour et al., 2015, 2011; Balistrieri et al., 2008; Ban et al., 2002; Bryan et al., 2015; Caldelas et al., 2011; Couder et al., 2015; Coutaud et al., 2014; Dong and Wasylenki, 2016; Fernandez and Borrok, 2009; Gélabert et al., 2006; Gou et al., 2018; Guinoiseau et al., 2016; Houben et al., 2014; Jamieson-Hanes et al., 2017; John et al., 2007a; John and Conway, 2014; Jouvin et al., 2012, 2009; Juillot et al., 2008; Kafantaris and Borrok, 2014; Nelson et al., 2017; Pokrovsky et al., 2005; Samanta et al., 2018; Smolders et al., 2013; Tang et al., 2016; Veeramani et al., 2015; Viers et al., 2007; Wanty et al., 2013; Weiss et al., 2005).

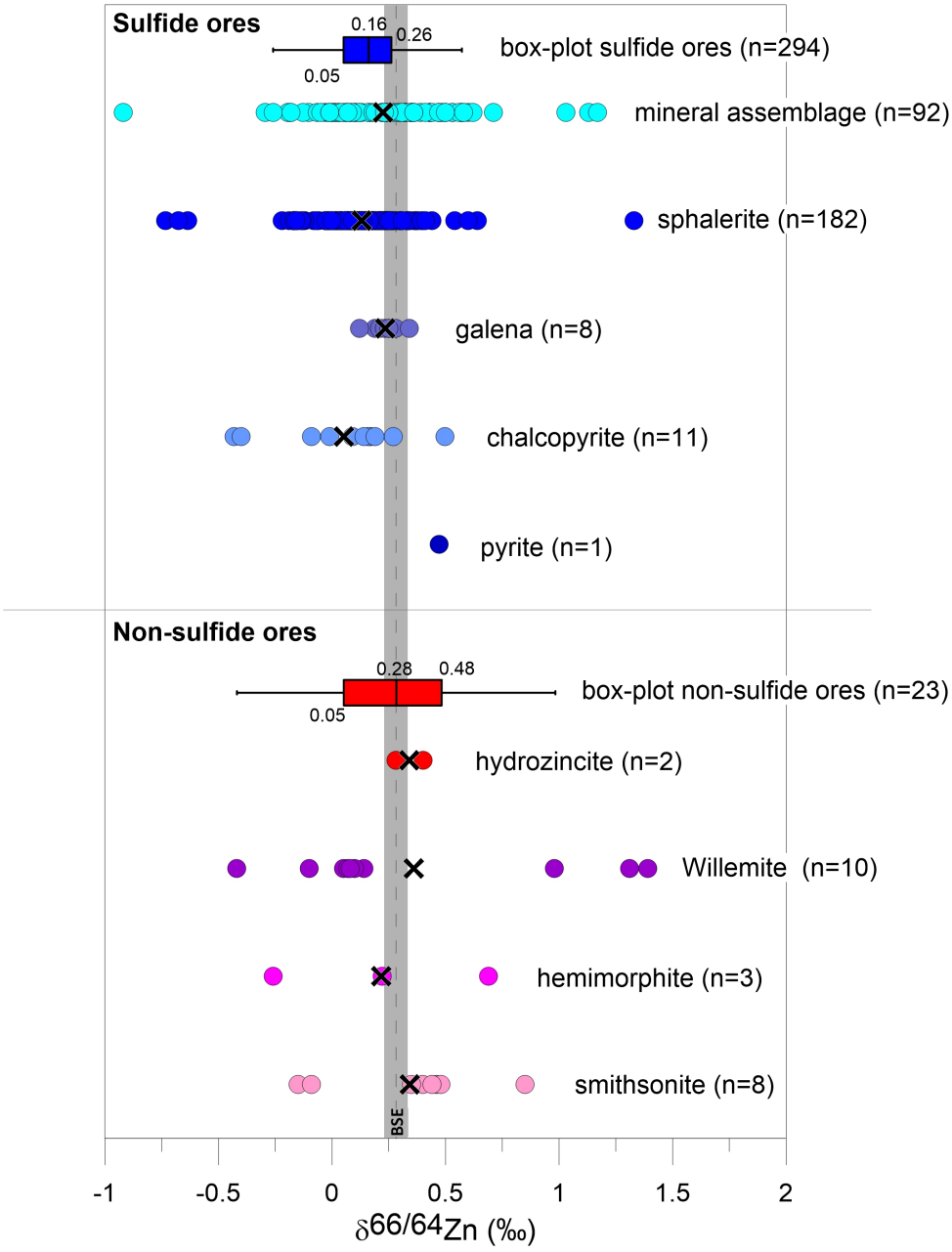

Fig. 2. Zinc isotope compositions for sulfide ores (n=294) and non-sulfide ores (n=23) (Aranda et al., 2012; Araújo et al., 2017a; Chapman et al., 2006; Deng et al., 2017; Duan et al., 2016; Gagnevin et al., 2012; John et al., 2008; Kelley et al., 2009; Maréchal et al., 1999; Mason et al., 2005; Mattielli et al., 2009; Mondillo et al., 2018; Novak et al., 2016; Pašava et al., 2014; Shiel et al., 2010; Sivry et al., 2008; Skierszkan et al., 2016; Sonke et al., 2008; Voldrichova et al., 2014; Wanty et al., 2013; Weiss et al., 2007; Wilkinson et al., 2005; Zhou et al., 2014). The mean value for each sample type is represented by a black cross. Box-plots are drawn for sulfide ore data in blue and for non-sulfide ore data in red. The vertical gray line labeled "BSE" is the mean of bulk silicate earth: 0.28 ± 0.05‰ (2σ) (Chen et al., 2013).

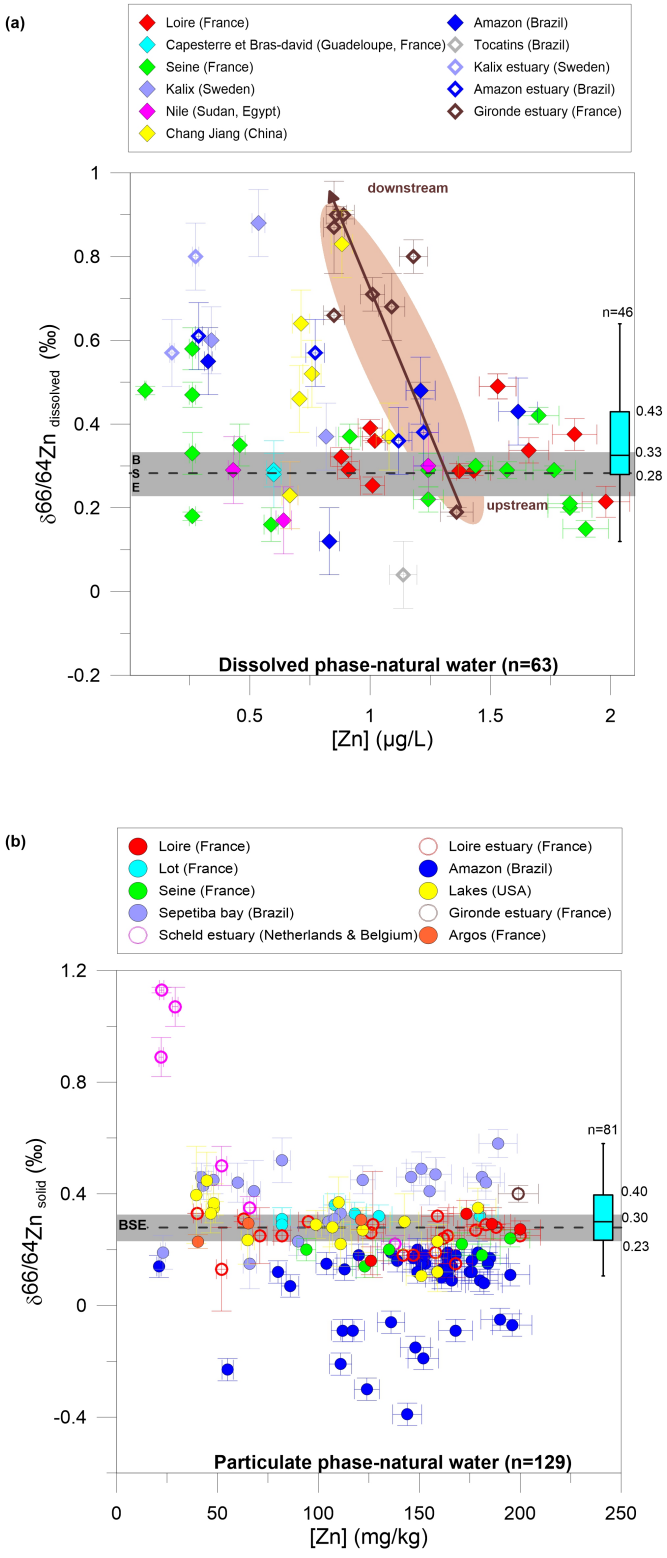

Fig. 3. $\delta^{66/64}$Zn value versus zinc content for dissolved zinc (n=63) and solid zinc (suspended particulate matter and sediment) (n= 129) in non-impacted rivers and lakes ($[Zn]_{dissolved} \leq 2$ µg/L, $[Zn]_{particulate} \leq 2$ µg/L) (Araújo et al., 2019, 2018, 2017a, 2017b; Chen et al., 2014, 2009b, 2008; Guinoiseau et al., 2018, 2017; Little et al., 2014; Petit et al., 2015, 2008; Sivry et al., 2008; Thapalia et al., 2015, 2010; this study). Error bars represent the 2σ associated with $\delta^{66/64}$Zn values. Data are also represented with blue box-plots for dissolved zinc in non-impacted rivers without estuary samples (n=46) and solid zinc in non-impacted rivers without Amazon samples (n=81).The horizontal gray line labeled "BSE" is the mean of Bulk Silicate Earth: 0.28 ± 0.05‰ (2σ) (Chen et al., 2013).

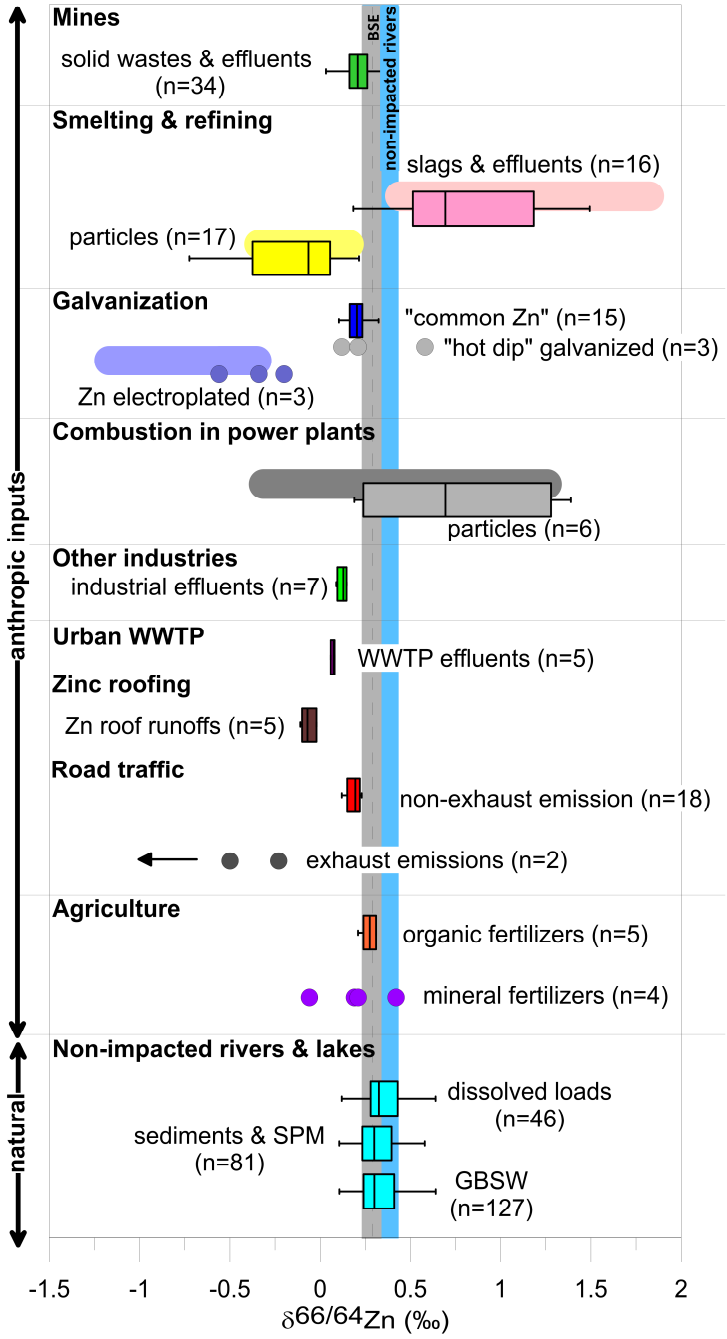

Fig. 4. Zinc isotope compositions for the various anthropogenic contributions: mining contribution (n=34), slags and slag effluents (n=16), particles zinc smelters (n=17), "common zinc" (n=15), particles in power plants (n=6), industrial effluents (n=7), WWTP effluents (=5), zinc roof runoff (n=5), non-exhaust road traffic emission (n=18) and organic fertilizer (n=5) are represented with box-plots (Aranda et al., 2012; Bigalke et al., 2010; Chen et al., 2008; Cloquet et al., 2006; Couder et al., 2008; Dong et al., 2017; Fekiacova et al., 2015; Gelly et al., 2019; John et al., 2007b; Juillot et al., 2011; Mattielli et al., 2009; Ochoa Gonzalez and Weiss, 2015; Shiel et al., 2010; Sivry et al., 2008; Skierszkan et al., 2016; Souto-Oliveira et al., 2018; Thapalia et al., 2010; Yin et al., 2018; this study). "Hot dip" galvanized materials (n=3), zinc electroplated hardware (n=3), exhaust road traffic emission (n=2) and mineral fertilizer (n=4) are represented by dot symbols (Chen et al., 2008; Gioia et al., 2008; Szynkiewicz and Borrok, 2016). The estimated values for slags and particles coming from zinc smelter, for electrogalvanized hardware and for particles issued from coal combustion and waste incineration are also represented with horizontal lines. Dissolved zinc in non-impacted rivers (n=46), solid zinc in non-impacted rivers (n=81) and "geological background for surface water" (GBSW) (n= 127) are represented by box-plots. The BSE value (+0.28 ± 0.05‰, 2σ) and the non-impacted river domain are represented by vertical lines (Chen et al., 2013).

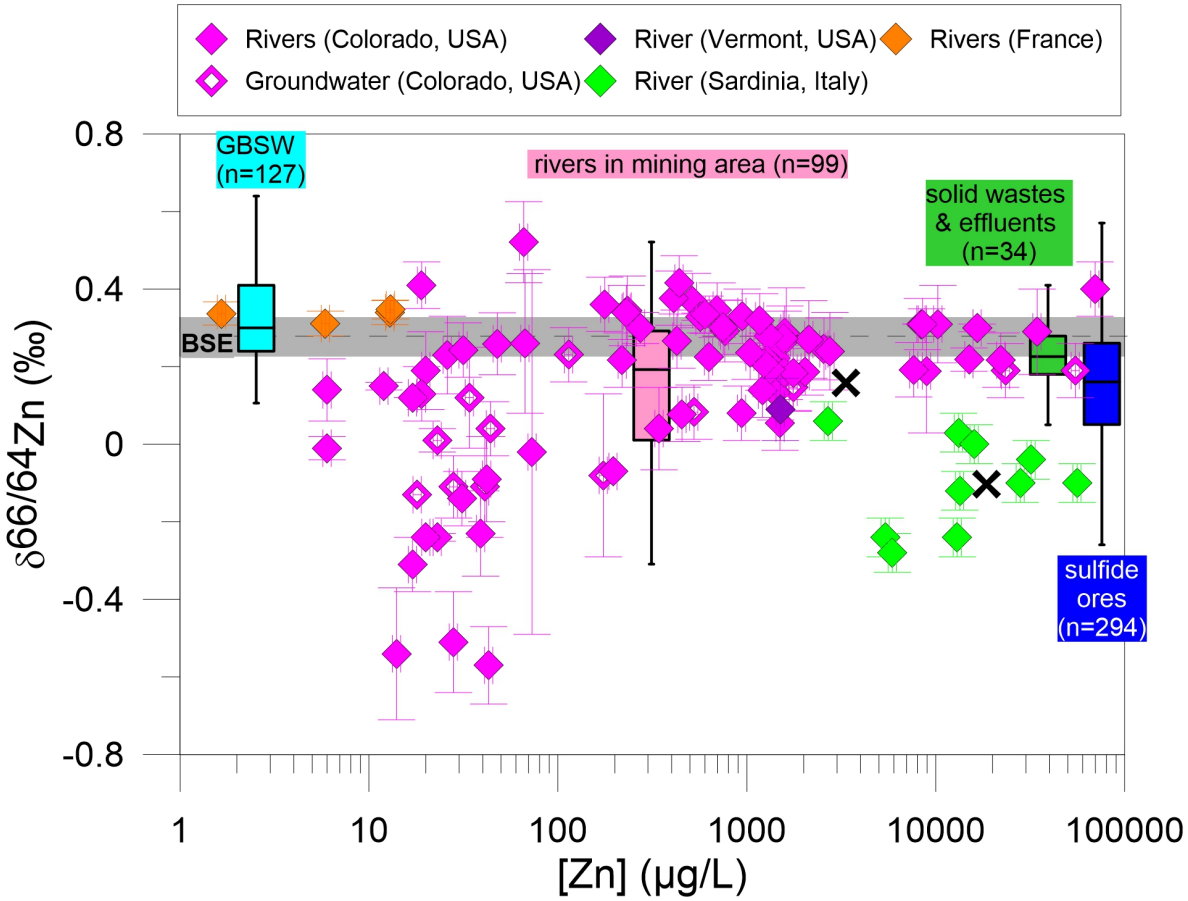

Fig. 5. $\delta^{66/64}$Zn value versus zinc content for dissolved zinc in rivers and groundwater in mining area (n=107) (Aranda et al., 2012; Balistrieri et al., 2008; Borrok et al., 2009; Szynkiewicz and Borrok, 2016; Wanty et al., 2013; this study). Error bars represent the 2σ associated with $\delta^{66/64}$Zn values. The mean value for each type of samples (USA & France, and Sardinia) is represented by a black cross. Data are represented with light blue box-plot for "geological background for surface water" (GBSW) (n= 127), pink box-plot for rivers and groundwater in mining area (n=107), with green box-plot for mining solid wastes and effluents (n=34) and with blue box-plot for sulfide ores (n=294).The gray line labeled "BSE" is the mean of bulk silicate earth: 0.28 ± 0.05‰ (2σ) (Chen et al., 2013).

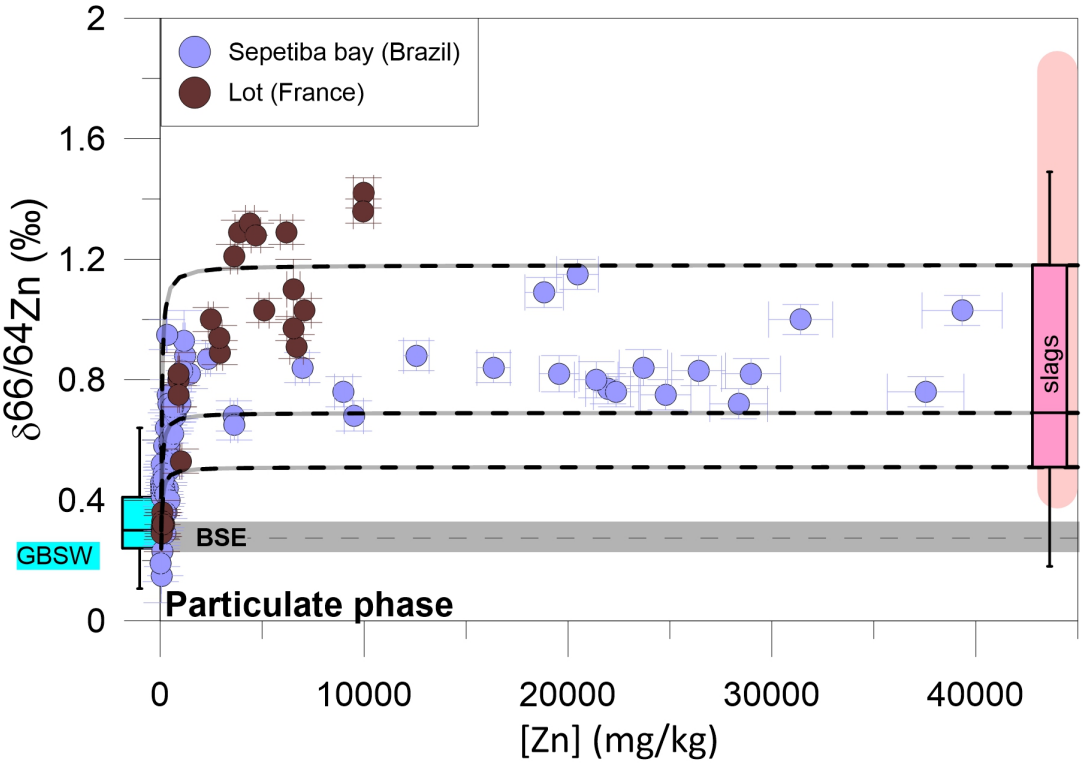

Fig. 6. $\delta^{66/64}$Zn value versus zinc content for sediments and suspended particulate matter in river and bay impacted by metallurgical industries (n=100)(Araújo et al., 2018, 2017a, 2017b; Petit et al., 2015; Sivry et al., 2008). Error bars represent the 2σ associated with $\delta^{66/64}$Zn values. Data are represented with light blue box-plot for "geological background for surface water" (GBSW) (n= 127) and pink box-plot for slag (n=11). The estimated values for slags are also represented with a pink line. The gray line labeled "BSE" is the mean of bulk silicate earth: 0.28 ± 0.05‰ (2σ) (Chen et al., 2013). The black dashed lines represent theoretical mixing lines between the range of values for "GBSW contribution" and for the "anthropogenic component" due to metallurgical activities (i.e. slags).

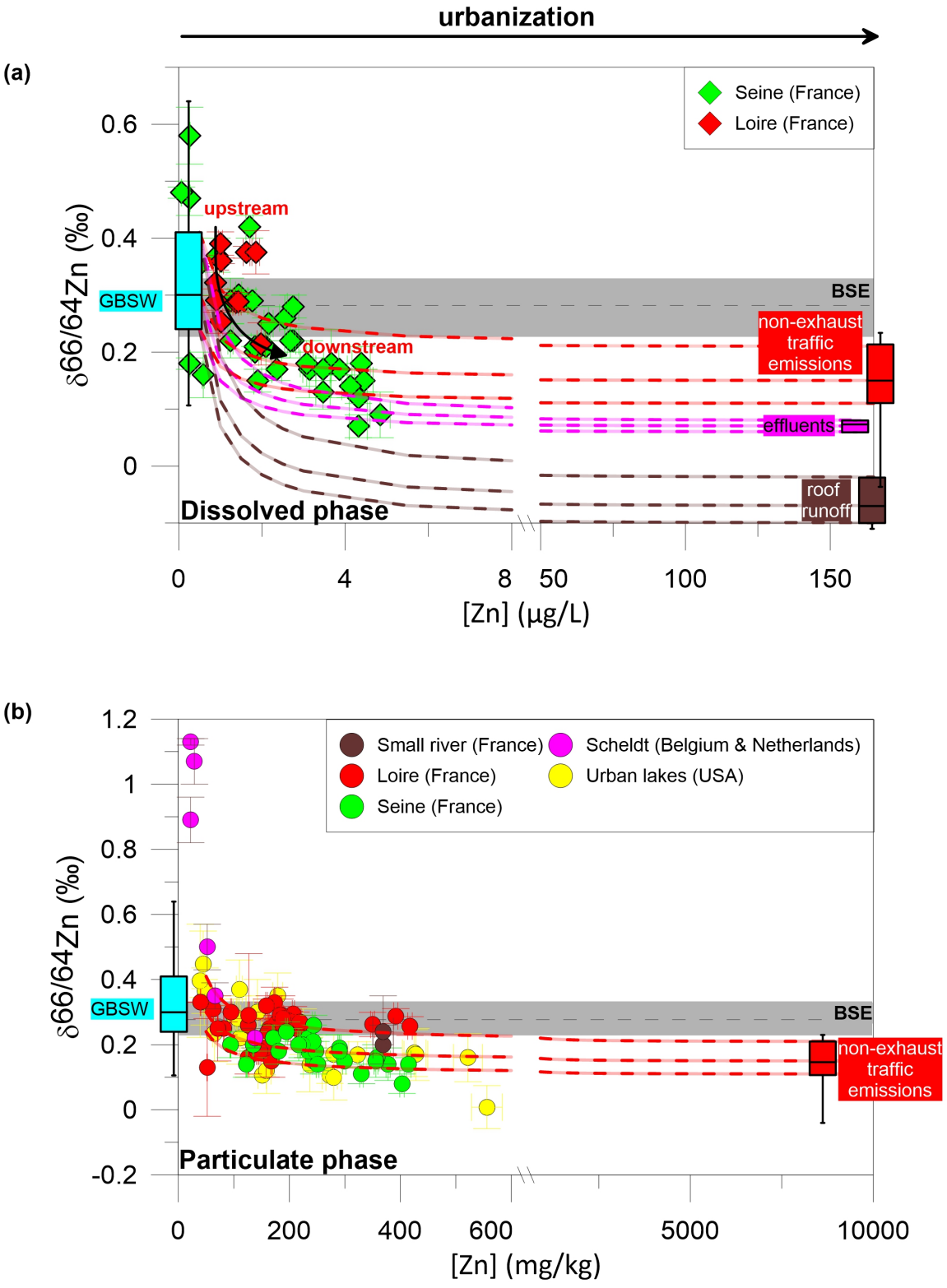

Fig. 7. $\delta^{66/64}$Zn value versus zinc content for urbanized rivers and lakes (a) dissolved load (n=46), (b) sediments and suspended particulate matter (n=96) (Araújo et al., 2019; Chen et al., 2009b, 2008; Petit et al., 2015, 2008; Thapalia et al., 2015, 2010; this study). Error bars represent the 2σ associated with $\delta^{66/64}$Zn values. Data are represented with light blue box-plot for "geological background for surface water" (GBSW) (n= 127), pink box-plot for WWTP effluents (n=5), brown box-plot for roof runoff (n=5), and red box-plot for non-exhaust road traffic emissions (n=18). The gray line labeled "BSE" is the mean of bulk silicate earth: 0.28 ± 0.05‰ (2σ) (Chen et al., 2013). The dashed lines represent theoretical mixing lines between the range of values for "GBSW contribution" and the "anthropogenic components" due to effluents, roof runoff and road traffic contributions.

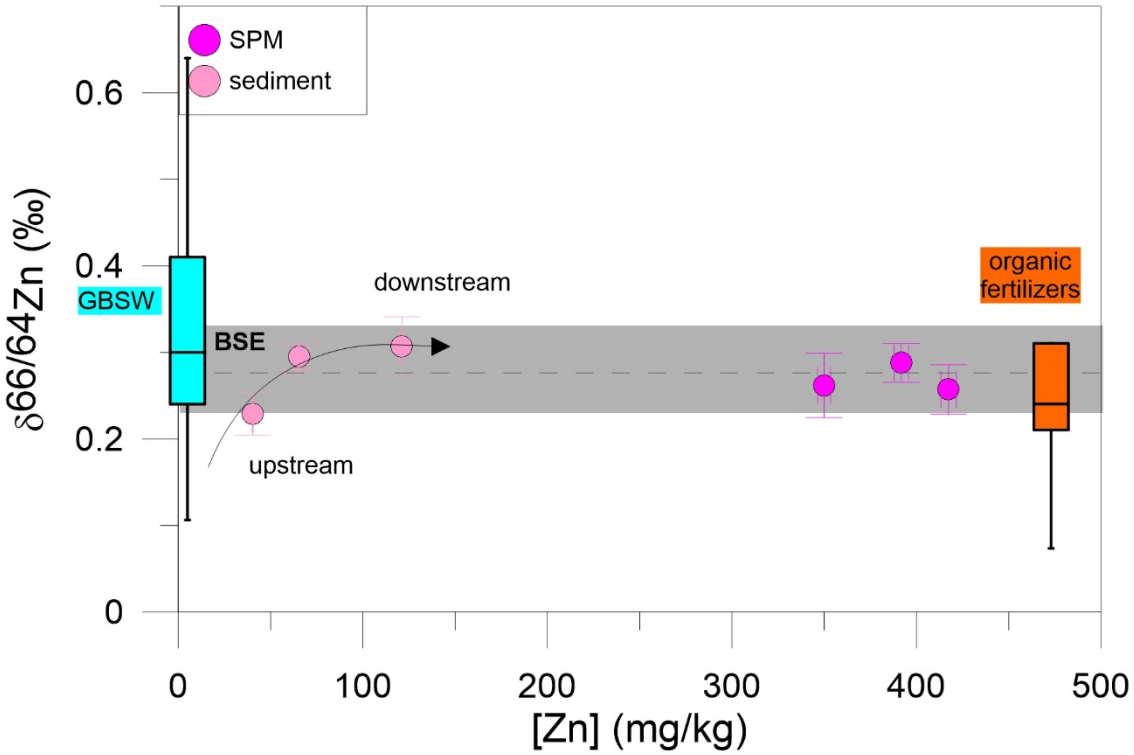

Fig. 8. $\delta^{66/64}$Zn value versus zinc content for sediments and suspended particulate matter in rivers impacted by agriculture activities (n=6) (this study). Error bars represent the 2σ associated with $\delta^{66/64}$Zn values. Data are represented with light blue box-plot for "geological background for surface water" (GBSW) (n= 127), and orange box-plot for organic fertilizer (n=5). The gray line labeled "BSE" is the mean of bulk silicate earth: 0.28 ± 0.05‰ (2σ) (Chen et al., 2013).

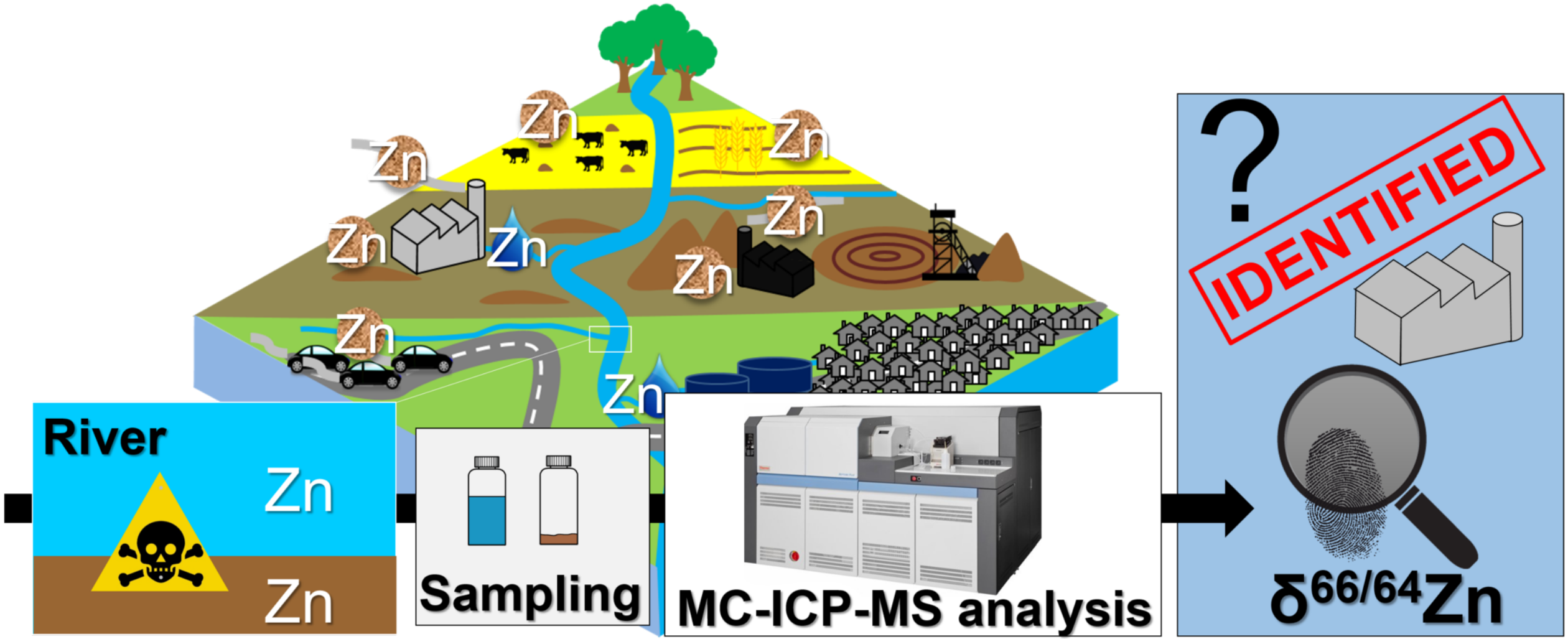
Zn
Zn
Zn
Zn
Zn
Zn
Zn
Zn
River
Zn
Zn
Sampling
MC-ICP-MS analysis
?
IDENTIFIED
δ66/64Zn